UNIVERSIDADE FEDERAL DO PARANÁ

LUCAS BOZZ BARBOSA

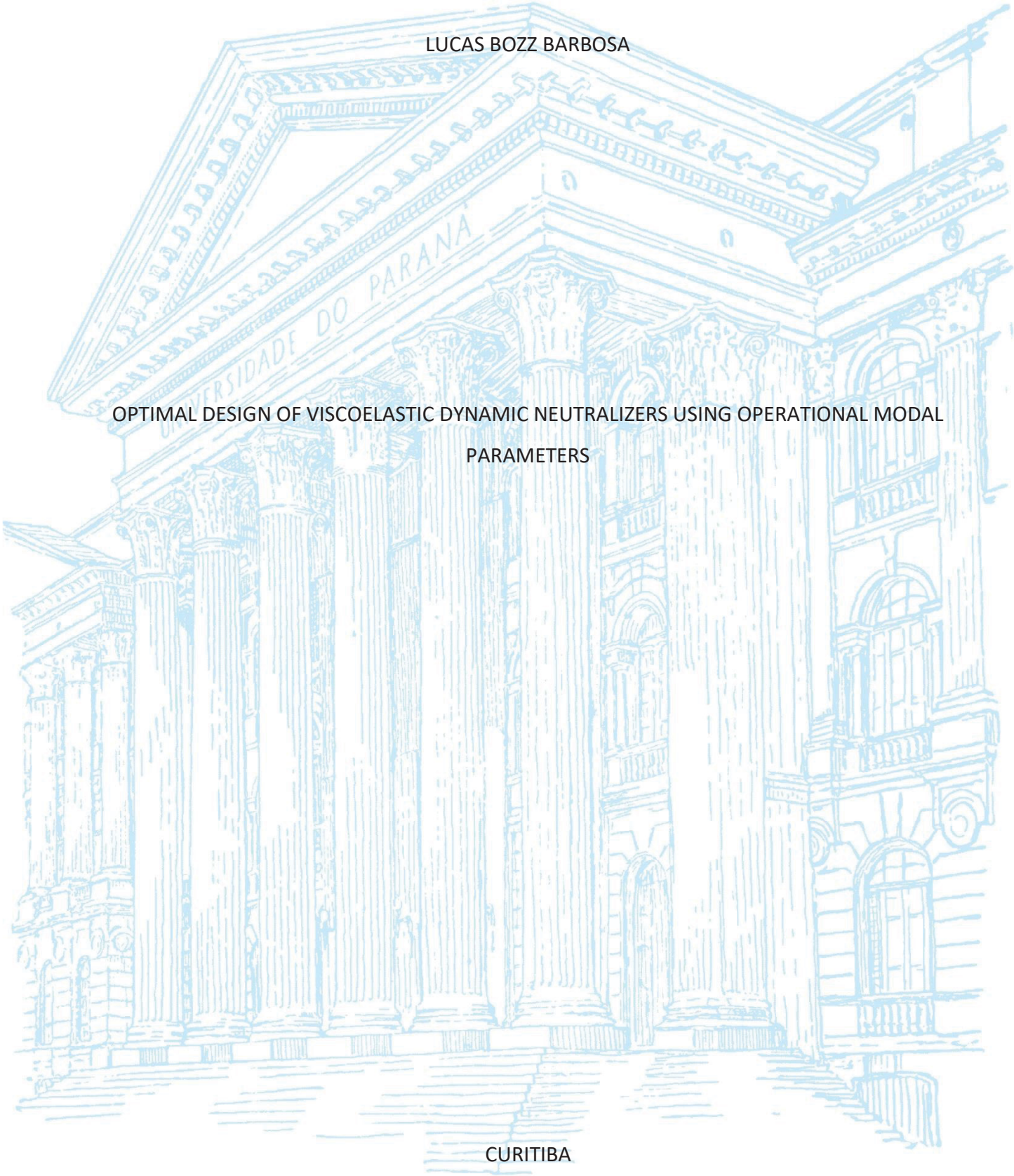

OPTIMAL DESIGN OF VISCOELASTIC DYNAMIC NEUTRALIZERS USING OPERATIONAL MODAL PARAMETERS

CURITIBA

2019

LUCAS BOZZ BARBOSA

OPTIMAL DESIGN OF VISCOELASTIC DYNAMIC NEUTRALIZERS USING OPERATIONAL MODAL PARAMETERS

Dissertação apresentada como requisito parcial à obtenção do grau de Mestre em Engenharia Mecânica, no Programa de Pós-Graduação em Engenharia Mecânica, Setor de Tecnologia da Universidade Federal do Paraná.

Orientador: Prof. Carlos Alberto Bavastri

Coorientador: Prof. Jörg Bienert

CURITIBA

2019

Catalogação na Fonte: Sistema de Bibliotecas, UFPR
Biblioteca de Ciência e Tecnologia

B238o Barbosa, Lucas Bozz
Optimal design of viscoelastic dynamic neutralizers using operational modal parameters [recurso eletrônico] / Lucas Bozz Barbosa. – Curitiba, 2019.

Dissertação - Universidade Federal do Paraná, Setor de Tecnologia, Programa de Pós-Graduação em Engenharia Mecânica, 2019.

Orientador: Carlos Alberto Bavastri – Coorientador: Jörg Blienert.

1. Materiais viscoelásticos. 2. Análise modal. 3. Pesquisa operacional. 4. Otimização estrutural . I. Universidade Federal do Paraná. II. Bavastri, Carlos Alberto. III. Blienert, Jörg. IV .Título.

CDD: 620.11232

Bibliotecário: Elias Barbosa da Silva CRB-9/1894

MINISTÉRIO DA EDUCAÇÃO
SETOR DE TECNOLOGIA
UNIVERSIDADE FEDERAL DO PARANÁ
PRÓ-REITORIA DE PESQUISA E PÓS-GRADUAÇÃO
PROGRAMA DE PÓS-GRADUAÇÃO ENGENHARIA MECÂNICA - 40001016040P5

TERMO DE APROVAÇÃO

Os membros da Banca Examinadora designada pelo Colegiado do Programa de Pós-Graduação em ENGENHARIA MECÂNICA da Universidade Federal do Paraná foram convocados para realizar a arguição da Dissertação de Mestrado de **LUCAS BOZZ BARBOSA** intitulada: **OPTIMAL DESIGN OF VISCOELASTIC DYNAMIC NEUTRALIZERS USING OPERATIONAL MODAL PARAMETERS**, sob orientação do Prof. Dr. CARLOS ALBERTO BAVASTRI, que após após terem inquirido o aluno e realizado a avaliação do trabalho, são de parecer pela sua APROVAÇÃO no rito de defesa.

A outorga do título de mestre está sujeita à homologação pelo colegiado, ao atendimento de todas as indicações e correções solicitadas pela banca e ao pleno atendimento das demandas regimentais do Programa de Pós-Graduação.

CURITIBA, 04 de Setembro de 2019.

CARLOS ALBERTO BAVASTRI
Presidente da Banca Examinadora (UNIVERSIDADE FEDERAL DO PARANÁ)

JUCÉLIO TOMAS PEREIRA
Avaliador Interno (UNIVERSIDADE FEDERAL DO PARANÁ)

MARIANO FEBBO
Avaliador Externo (UNIVERSIDAD NACIONAL DEL SUR)

RESUMO

Em muitos casos, a vibração é um efeito indesejável que resulta em desconforto ou até falha de uma estrutura. Um projeto cuidadoso pode atenuar esses efeitos, mas isso nem sempre é possível. Uma solução simples é o uso de 'neutralizadores dinâmicos de vibração' - simplesmente conhecidos como 'neutralizadores dinâmicos' (ND's). Estes são dispositivos que reduzem as vibrações quando conectados a uma estrutura. Os neutralizadores iniciais eram limitados em suas aplicações, pois eram projetados para um único modo em uma estrutura relativamente simples. A introdução de teorias matemáticas mais modernas, bem como a introdução de materiais viscoelásticos, permitem um design mais robusto com uma maior variedade de aplicações, em particular, o 'neutralizador dinâmico viscoelástico' (NDV). A utilização de técnicas de otimização não lineares garante a máxima eficiência desses dispositivos. Trabalhos anteriores desenvolveram e apresentaram uma metodologia geral para projetar NDV's para um sistema primário linear, usando seus parâmetros modais experimentais como entrada e conceitos como parâmetros equivalentes generalizados e técnicas de otimização não linear. O objetivo do presente trabalho é testar a metodologia atual com parâmetros modais operacionais e comparar os resultados com os obtidos com os parâmetros modais experimentais, a fim de garantir sua eficácia.

Palavras-chave: Neutralizadores dinâmicos. Materiariais viscoelasticos. Análise modal experimental. Análise modal operacional. Otimização.

ABSTRACT

In many cases, vibration is an undesirable effect that results in discomfort or even failure of a structure. A careful design can mitigate these effects, but that is not always possible. A simple solution is the use of 'dynamic vibration neutralizers' (DVN) - simply known as 'dynamic neutralizers' (DN). They are devices that reduce vibrations when attached to a structure. Early neutralizers were limited in their applications, since they were designed for a single mode in a relatively simple structure. The introduction of more modern mathematical theories as well as the introduction of viscoelastic materials allow for a more robust design with a greater range of applications, namely the 'viscoelastic dynamic neutralizer' (VDN). The utilization of nonlinear optimization techniques ensures maximum efficiency of these devices. Previous works have developed and presented a general methodology for designing VDN's for a linear primary system, using its experimental modal parameters as input and concepts such as generalized equivalent parameters and nonlinear optimization techniques. The aim of the present work is to test the current methodology with operational modal parameters and compare the results with those obtained with the experimental modal parameters in order to assure its efficacy.

Keywords: Dynamic neutralizers. Viscoelastic materials. Experimental modal analysis. Operational modal analysis. Optimization.

CONTENTS

LIST OF FIGURES

LIST OF TABLES

1. INTRODUCTION

Dynamic Vibration Neutralizers, often called ‘Dynamic Vibration Absorbers’ - or simply ‘Dynamic Neutralizers’ (DN) -, are mechanical devices to be attached to another mechanical system, or structure - called ‘primary system’ - with the purpose of reducing or controlling vibrations and sound radiation. Viscoelastic dynamic neutralizers (VDN) are easy to build and apply to structures of any sizes and shapes. To a certain extent, this is possible thanks to the modern technology regarding viscoelastic materials, which makes it easy to mold them in any shape and tailor it to meet almost any specifications.

In Espíndola and Silva (1992), a general theory was derived for the optimum design of neutralizer systems, when applied to a generic structure in any amount. This theory can be used for any kind of neutralizer, but emphasizes the optimum design of viscoelastic neutralizers, as presented in Bavastri (1997), Espíndola et al. (2005a), and Espíndola et al. (2008). It is based on the concept of ‘equivalent generalized mass’ and ‘damping parameters’ for the absorbers and on an equivalent Den Hartog methodology for a single-degree-of-freedom (SDOF) primary system, in which the modes are controlled individually. However, starting with Bavastri (1997), the control can be made in a broad band of frequencies, where one or more neutralizers can control one or more vibration modes, thanks to the use of nonlinear optimization techniques.

As part of the problem, it is necessary to know the modal parameters of the primary system, which can be obtained through experimental modal analysis (EMA), operational modal analysis (OMA), or finite elements analysis (FEA). The developed formulation assumes that the mode shapes are orthonormalized by the modal mass of the system, the way they are when obtained by experimental modal analysis, which is not true for operational modal analysis. The main objective of the present work is to show that the existing formulation can be used with operational modal parameters as input.

1.1. OBJECTIVES

The primary objective of the present work is to test and validate the existing methodology for the design of VDN using operational modal parameters. This is achieved by comparing the results obtained from both experimental and operational analyses.

The secondary objective is (i) to obtain both modal analysis parameters for an aluminum frame, (ii) design one set of neutralizers for each, and (iii) compare the numerical and experimental results obtained from each set.

2. LITERATURE REVIEW

This chapter is dedicated to the presentation of the themes of the present project focusing on dynamic vibration neutralizers and viscoelastic materials (VEM). Such devices date back from at least 1909 and have been subjects of study in the field of mechanical vibrations since then. The first devices did not present damping and were, thus, narrowband control devices. With modern viscoelastic materials, it is possible to achieve broadband control with cheap and compact devices.

2.1. SINGLE-DEGREE-OF-FREEDOM DYNAMIC NEUTRALIZER

Dynamic neutralizers are simple systems which, when attached to a mechanical structure, reduce its vibration levels. In its simplest form, it is a tuned mass attached to a primary structure by a resilient element - a spring, for example. In this form, the neutralizer is known as a 'narrow band neutralizer'. As demonstrated by Den Hartog (1956), the vibration of the primary system can approach zero when the natural frequency of the neutralizer is equal to that of the system.

If the connection presents any kind of damping, then the neutralizer fits the category of 'broad band neutralizers'. The classical method for this kind of DN's is known as the 'fixed point method', developed by Den Hartog (1956). This method considers: (1) an undamped primary structure and (2) that there are two points in which the response of the compound system (primary system plus neutralizer) coincides with the response of the primary structure. According to the author, the most effective tuning of the neutralizer is observed when the maximums of the response are equal and coincide with the fixed points. This method calculates not only the optimal natural frequency of the neutralizer, but also the damping coefficient.

However, this theory is limited and better suited for an SDOF primary system. For more complex systems, more vibration modes contribute to the response of the structure and, thus, a more robust methodology is required.

The first recorded case of a dynamic vibration neutralizer dates back to 1909, when Frahm patented a device for damping vibration in bodies, more specifically, ships. In the patent document, he states that the device should have as close as possible the resonance

frequency of the main body. However, it was only in 1928, that Ormondroyd and Den Hartog addressed the issue in mathematical depth. Later, in 1956, Den Hartog presented the Fixed Point Theory, which determines the optimum resonance frequency and damping ratio for a dynamic absorber in a single-degree-of-freedom primary system. Espíndola and Silva (1992) proposed the equivalent generalized parameters, which represent the compound system in terms of the generalized coordinates of the primary system only. This further increases the generality of DN's. Like Ormondroyd and Den Hartog, the control of the modes was performed one at a time.

For a simultaneous control of multiple modes, a more robust technique becomes necessary. The use of nonlinear optimization techniques is presented by Kitis (1983), in which he considers a system of n degrees of freedom in the primary system and p neutralizers, resulting in n + p equations. This allows for a multiparameter optimal design of one or more neutralizers. By formulating the objective function as the Euclidean norm of the response over a frequency range, Bavastri and Espíndola (1995) used this concept in conjunction with the generalized equivalent to optimally design dynamic neutralizers for a broadband control using a reduced number of equations.

The field of DN's is the subject of constant study and development. Huang and Lin (2014) analyze several existing designs for DN's and then propose a new one called 'periodic vibration absorber' (PVA). Even with the more traditional designs, developments are being made regarding global control using a single (Brennan and Dayou (2000)) or multiple neutralizers (Dayou and Brennan (2002)).

2.2. VISCOELASTIC MATERIALS

Viscoelastic materials are largely used as a means to provide damping to structures, thus mitigating resonant vibration responses. Devices made with viscoelastic materials - such as isolators, dynamic neutralizers, sandwich panels, and structural links - can be designed for highly efficient vibration control. In order to properly devise a vibration control strategy with viscoelastic materials, two basic dynamic properties must be known: the material loss factor and the dynamic modulus of elasticity. They are also widely used for noise control. Rao (2003) presents a number of possible applications in automobiles and commercial airplanes.

Theoretical analyses of the VEM mechanism can be traced back to the 1950's. Snowdon (1959) presented an analysis of a SDOF neutralizer which consisted of - as he defined it - a rubber–like material, and not with a spring and dashpot in parallel, as considered in the classical theory by Ormondroyd and Den Hartog (1956). Having a material with a stiffness proportional to frequency and a constant damping factor, this dynamic neutralizer could considerably reduce the resonant vibration of machinery and equipment items. It has shown a superior performance to that of the classical dynamic neutralizer.

In the past, the rheological model for viscoelastic materials was based on the classical concept of derivative (with respect to time) of integer order. These constitutive equations contained too many parameters to be identified, which rendered the task computationally impractical. More recent studies present an alternative method for identifying viscoelastic materials, the fractional (or generalized) derivative, presented in Bagley and Torvik (1979), Torvik and Bagley (1983), Bagley and Torvik (1986), Padovan and Guo (1988), Pritz (1998), Kim and Lee (2009), among others.

The exact modeling of a viscoelastic material is difficult, mainly because its dynamic parameters are significantly affected by frequency and temperature. Zhou et al. (2016) review multiple theoretical models used to describe it. The fractional derivative model (FDM) has proved to be effective and useful in the research of the dynamic properties of the VEM structures in the frequency domain. Its most important feature is its ability to capture the frequency dependency using few model parameters, usually from three to six. Eldred et al. (1995) validated the FDM with an experimental measurement of the loss factor and elastic modulus, and also showed that a four-parameter FDM improves the accuracy of VEM modeling when compared to the three-parameter FDM. Bavastri (1997) used this type of material on a neutralizer to control a thin steel plate and validated the general methodology for a frequency broadband control by comparing experimental and theoretical results. Olienick Filho et al. (2017) used fractional derivatives for the characterization of the butyl rubber, but also including the effects of a static load (preload) on the material characterization.

The model used for the present work is the one presented in Espíndola et al. (2005a), using only four parameters, considering its properties as functions of frequency and temperature.

For the passive control of vibrations in particular, Snowdon (1968) first presented the viscoelastic model as a replacement for the usual spring and damper link. His work, like many others that came after it - Nashif and Jones (1969), Jones et al. (1975), Snowdon and Nobile (1980), and Snowdon et al. (1984), to mention a few - was for a SDOF primary system or an equivalent SDOF system. Beginning with Espíndola and Silva (1992), his generalized equivalent parameters formulation allowed for a multiple-degrees-of-freedom (MDOF) primary system.

2.3. OPERATIONAL MODAL ANALYSIS

Modal analysis is the field of engineering responsible for identifying the dynamic behavior of bodies and structures from the measured excitations and responses. The results of a modal analysis are the modal parameters (natural frequencies, mode shapes, and modal dampings), which are related to the physical and mechanical properties of the analyzed structure, such as mass, stiffness, and energy dissipation.

Operational modal analysis - or simply OMA - is a fairly recent field of study. Although some studies in the field date back to the 1930's, it was in the 1990's that OMA saw its more significant advances. While EMA is based on the fact that both excitation and response of a vibrating system are measured, in OMA only the response is known. Excitation is considered to be a white noise, and thus the parameter estimation methods are based on signal processing concepts, such as power spectral density. Brincker (2014) presents the main components of OMA, such as the Fourier series, the Fourier integral, the Laplace transform, and the Z-transform.

The identification methods for OMA can be either in the time domain or the frequency domain. The most common technique for the time domain is the stochastic subspace identification (SSI) and its variants, by Van Overschee and De Moor (1996), which borrows heavily from the Control Theory. The most common method for the frequency domain is the frequency domain decomposition (FDD) by Brincker et al. (2000) and its variants. This method considers that each mode has a narrow band of frequency where a mode dominates. Another method for the frequency domain that has gained popularity in the early 2000's is the PolyMax, presented by Guillame et al. (2003).

As the name implies, operational modal analysis is performed with the structure under operating conditions and, thus, it is possible in cases where EMA is not always possible,

such as in large and complicated structures, like aerospace structures (Eugeni et al. (2017)), industrial plants (Schneider (2017)), or civil structures (Brincker and Andersen (2000)).

It is well known that the two main disadvantages of OMA are the lack of mass scaling of the modes and the eventual lack of excitation of some modes. Because it is not possible to measure the input force when using ambient excitation, the identification process does not provide either mass normalized mode shapes or the frequency response functions (FRF). There are, however, separate tests that may provide the modal mass or the mass normalized modes directly (Lopez-Aenlle et al. (2005), Parloo et al. (2002), and Khatibi et al. (2012)).

3. THEORY

For the present work, it is important to understand the concepts of viscoelastic materials and models, dynamic neutralizers, and nonlinear optimization techniques. Such concepts will be presented in this chapter in order to properly define the problem and, subsequently, present a solution.

3.1. LINEAR VISCOELASTICITY

Purely elastic materials deform in function of the applied stress. There are two fundamental types of deformations: longitudinal strains (traction and compression), where the material suffers a variation in volume, but not shape; and shear strains, where the material changes its shape, but not its volume.

For materials with linear isotropic behavior, the relation between its longitudinal and shear deformations is defined by the Poisson ratio:

$$\nu = -\frac{d\varepsilon_{trans}}{d\varepsilon_{axial}} = \frac{E}{2G} - 1 \tag{3.1}$$

In general, for viscoelastic materials, the Poisson ratio ranges from approximately $\nu \approx 0.4$ to 0.5 (de Sousa (2018)). Given the temperature and operating frequencies in this project, the best approximation is $\nu \approx 0.5$. That means, according to equation (3.1), $E \approx 3G$. That is a very important relation for the design of DN's since their construction can be based on either longitudinal deformations or shear deformations. It is also important to note that viscoelastic materials present a relatively high Poisson ratio, so the lateral bulge of compression springs must be taken into consideration, otherwise the necessary flexibility cannot be achieved.

When a viscoelastic linear material is subject to time variant stress and strains, they cannot be related through simple proportionality constants (such as G). This behavior is better described by a partial differential equation of arbitrary order, given by

$$\sigma(t) + \sum_{m=1}^{M} b_m \frac{d^m \sigma(t)}{dt^m} = E_0 \varepsilon(t) + \sum_{n=1}^{N} E_n \frac{d^n \varepsilon(t)}{dt^n} \tag{3.2}$$

where b_m, with $m = 1 \dots M$, E_0 and E_n, with $n = 1 \dots N$, are material parameters, constants in time, $\sigma(t)$ is the stress time history, and $\varepsilon(t)$ is the strain time history. Fourier transforming both sides and rearranging leads to the complex elastic modulus $E_c(\Omega)$

$$E_c(\Omega) = \frac{\sigma(\Omega)}{\varepsilon(\Omega)} = \frac{E_0 + \sum_{n=1}^{N} E_n \, (i\Omega)^n}{1 + \sum_{m=1}^{M} b_m \, (i\Omega)^m} \tag{3.3}$$

where $\sigma(\Omega)$ and $\varepsilon(\Omega)$ are the stress and strain in the frequency domain, respectively.

Equivalently, the shear modulus $G_c(\Omega)$ can be represented by

$$G_c(\Omega) = \frac{\tau(\Omega)}{\gamma(\Omega)} = \frac{G_0 + \sum_{n=1}^{N} G_n \, (i\Omega)^n}{1 + \sum_{m=1}^{M} b_m \, (i\Omega)^m} \tag{3.4}$$

where $\tau(\Omega)$ and $\gamma(\Omega)$ are the shear stress and strain in the frequency domain, respectively.

This model, however, requires too many parameters to accurately represent the real behavior of the viscoelastic material, which can be computationally impractical. In Espíndola et al (2005a), a new model, based on fractional derivatives, was used to accurately represent the material with as few as four parameters.

3.1.1. Fractional derivatives model

Let a function $f(x)$ be infinitely differentiable, a derivative of order n is the nth derivative of the function, where n is an integer – negative values of n are the antiderivatives of the function. The operator $D^n[f(x)]$ represents the derivative of order n of the function – many other notations exist, but this will be used for its practicality.

Fractional differential equations are a generalization of differential equations, where instead of $\{D^n | n \in \mathbb{Z}\}$, the more general $\{D^\alpha | \alpha \in \mathbb{R}\}$ is used. Among the several different definitions of fractional derivatives, Espíndola et al (2005a) and Espíndola et al (2005b) use the Riemann-Liouville definition

$$D^\alpha[f(t)] = \frac{1}{\Gamma(1-\alpha)} \frac{d}{dt} \int_0^t \frac{f(\tau)}{(t-\tau)^\alpha} d\tau \tag{3.5}$$

where α is the fractional order of the derivative and $\Gamma(\cdot)$ is the gamma function.

A known property of fractional derivative and Fourier transform is that:

$$\mathcal{F}\{D^\alpha[f(t)]\} = (i\Omega)^\alpha \mathcal{F}[f(t)] = (i\Omega)^\alpha F(\Omega) \tag{3.6}$$

where $\mathcal{F}[f(t)]$ is the Fourier operator, and $F(\Omega)$ is the Fourier transform of function $f(t)$.

Thus, in its most general form, the constitutive equation that describes the behavior of viscoelastic materials in terms of fractional derivatives is

$$\sigma(t) + \sum_{m=1}^{M} b_m D^{\beta_m}[\sigma(t)] = E_0\varepsilon(t) + \sum_{n=1}^{N} E_n D^{\alpha_n}[\varepsilon(t)] \tag{3.7}$$

Similar to the model of integer order, b_m, β_m, with $m = 1 \dots M$, E_0, E_n and α_n with $n = 1 \dots N$ are material parameters, constants in time; $\sigma(t)$ is the stress time history; and $\varepsilon(t)$ is the strain time history. Although this model is very similar to the one mentioned before, it can achieve better results with as few as four parameters.

For this project, a four-parameter model is used

$$\bar{E}(\Omega) = \frac{E_0 + E_\infty(i\Omega)^\alpha}{1 + b(i\Omega)^\alpha} \tag{3.8}$$

The same process can be used to obtain a model for the shear modulus.

$$\bar{G}(\Omega) = \frac{G_0 + G_\infty(i\Omega)^\alpha}{1 + b(i\Omega)^\alpha} \tag{3.9}$$

Quantity $\bar{E}$ is the complex elastic modulus and can be rewritten in its complex and imaginary parts:

$$\bar{E}(\Omega) = E_r(\Omega) + iE_i(\Omega) \tag{3.10}$$

where E_r and E_i are its real and imaginary parts, respectively. It is important to note that the elastic modulus is a function of both frequency Ω and temperature θ. However, the temperature will be considered constant, so the modulus will be expressed as a function of frequency only. Similarly, in the case of a pure shear, the shear modulus can be expressed by:

$$\bar{G}(\Omega) = G_r(\Omega) + iG_i(\Omega) \tag{3.11}$$

The real part corresponds to the stored elastic energy, whereas the imaginary part is the energy dissipation. Another representation for these equations is through the loss factor η, which is the ratio between the dissipated energy and the stored energy.

$$\bar{E}(\Omega) = E_r(\Omega)(1 + i\eta_E(\Omega)) \tag{3.12}$$

$$\bar{G}(\Omega) = G_r(\Omega)(1 + i\eta_G(\Omega)) \tag{3.13}$$

where

$$\eta_E(\Omega) = \frac{E_i(\Omega)}{E_r(\Omega)} \tag{3.14}$$

$$\eta_G(\Omega) = \frac{G_i(\Omega)}{G_r(\Omega)} \tag{3.15}$$

According to Snowdon (1968), for rubbers in general and some metals, $\eta_E(\Omega) = \eta_G(\Omega)$.

While G and E are intensive material properties (not dependent on shape or size), stiffness K is an extensive property, that is, it is dependent on shape and size. The stiffness and shear moduli of a viscoelastic material are related by

$$K(\Omega) = L\bar{G}(\Omega) \tag{3.16}$$

where L is a geometric factor for the ideal shear case is given by

$$L = A/h \tag{3.17}$$

Other cases, such as pure compression or combined load modes have different geometric factors. Those are explained in depth in Nashif et al. (1985).

3.1.2. Dependence on temperature

From equations (3.8) and (3.9), it is clear the dependency of the moduli on frequency. However, none of the previous equations clarifies the dependency of the material parameters on temperature and, consequently, on the complex moduli.

Viscoelastic materials follow a general pattern called 'principle of frequency-temperature superposition'. It states that $\log\big(G_r(\Omega)\big)$ and $\log\big(\eta(\Omega)\big)$ versus $\log(\Omega)$, at any temperature, are similar enough to be considered the same, but displaced along the frequency axis. This principle is the basis for the construction of the nomograms (Figure 3.1) known as the 'reduced frequency plot'. In this nomogram, the plots for the various temperatures are represented by a single reference plot for an arbitrarily selected reference temperature T_0. Then, with the assistance of guide lines for the temperatures, the corresponding shifted values for modulus and loss factor can be obtained, as follows:

$$\bar{E}(\Omega, T) = \frac{E_0 + E_\infty (i\, s(T)\Omega)^\beta}{1 + b(i\, s(T)\Omega)^\beta} \tag{3.18}$$

$$\bar{G}(\Omega, T) = \frac{G_0 + G_\infty (i\, s(T)\Omega)^\beta}{1 + b(i\, s(T)\Omega)^\beta} \tag{3.19}$$

$$\log[s(T)] = -\frac{\theta_1(T - T_0)}{\theta_2 + (T - T_0)} \tag{3.20}$$

Function $s(T)$ is the shift function. It is used to compute the values for $\bar{E}$ and $\bar{G}$ at different temperatures T. Product $s(T)\,\Omega$ is the reduced frequency Ω_r. Parameters θ_1 and θ_2 of the displacement function (3.20) are constants to be determined experimentally. If the temperature chosen is $T = T_0$, it is trivial that $s(T_0) = 1$, and so, $\Omega_r = \Omega$.

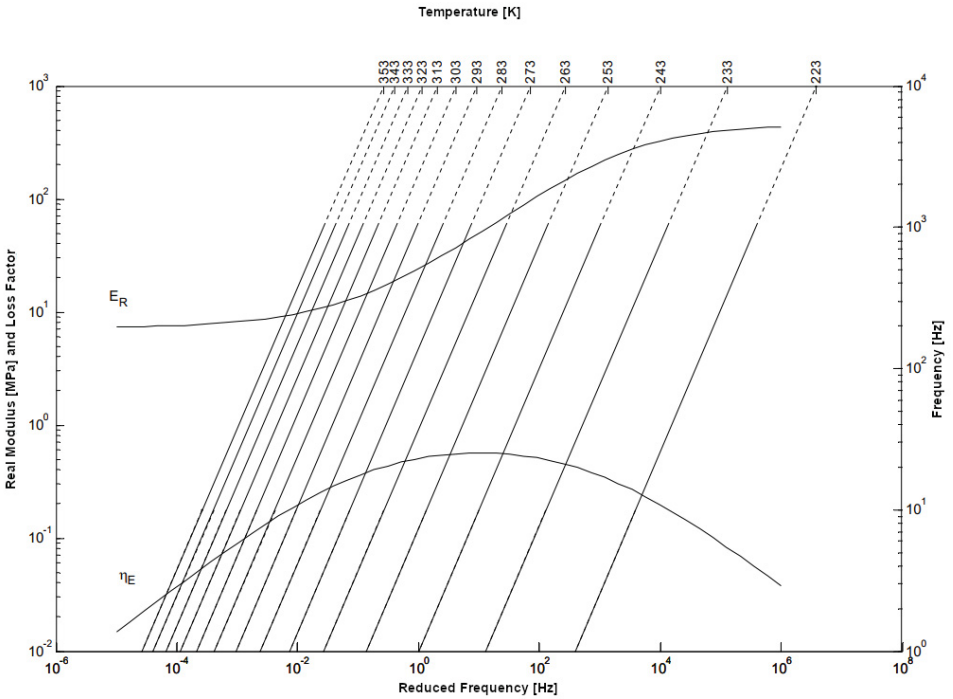

Figure 3.1 – Nomogram for the BT-806/55 rubber. Source: The Author.

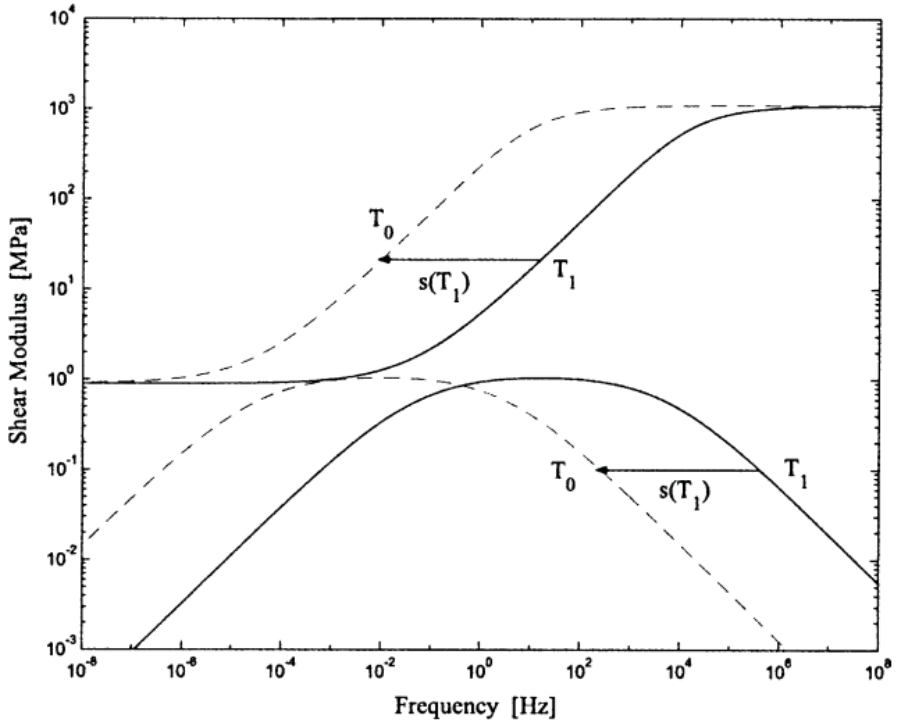

Figure 3.2 – Behavior of the modulus and loss factor at T_0 and T_1. Source: adapted from Espíndola et al. (2005b).

The shift function allows for the computation of the values for modulus and loss factor at any temperature given that the curves at the reference temperature and the coefficients of the displacement function are known.

3.2. SINGLE-DEGREE-OF-FREEDOM VIBRATION

A system is said to be single-degree-of-freedom (SDOF) if it is fully described by a single coordinate, for example, a rigid body moving in a prismatic joint, such as a piston. Realistically, very few practical structures can be modeled as an SDOF system; however, in some cases, a multi-degree of freedom (MDOF) problem can be simplified to an equivalent SDOF problem, like a cantilever beam with a concentrated mass in the free end. Another importance of the study of SDOF systems is that the MDOF systems can be represented as a superposition of SDOF characteristics. Dynamic neutralizers can also be represented as SDOF systems. A more detailed explanation can be found in Ewins (1984), Rao (2004) and Inman (2014).

There are three major classifications for SDOF systems regarding the damping type:

a) undamped;

b) viscously-damped;

c) histeretically- (or structurally-) damped.

Regarding the type of vibration of the system, it can be classified as:

a) free-vibration;

b) forced-vibration.

The damped single-degree-of-freedom system with free vibration can be described as a mass-spring-damper system. The equation of movement is obtained by the free body diagram analysis

$$m\ddot{x}(t) + c\dot{x}(t) + kx(t) = 0 \tag{3.21}$$

In order to reach the solution, the trial solution $x(t) = Ce^{st}$ is used. Substituting it back into (3.21) leads to

$$ms^2 + cs + k = 0 \tag{3.22}$$

in which the roots for s are

$$s_{1,2} = -\frac{c}{2m} \pm \sqrt{\left(\frac{c}{2m}\right)^2 - \frac{k}{m}} \tag{3.23}$$

By defining the critical damping c_c as the value of c, in which the square root becomes null, and the damping ratio as $\zeta = c/c_c$, the following equation is true

$$c_c = 2m\,\Omega_n \tag{3.24}$$

where Ω_n is the natural frequency of the system. And

$$\frac{c}{2m} = \frac{c}{c_c}\frac{c_c}{2m} = \zeta\,\Omega_n \tag{3.25}$$

so the roots of s can be rewritten as

$$s_{1,2} = \left(-\zeta \pm \sqrt{\zeta^2 - 1}\right)\Omega_n \tag{3.26}$$

and the general solution for equation (3.21) is

$$x(t) = C_1 e^{s_1 t} + C_2 e^{s_2 t} \tag{3.27}$$

where C_1 and C_2 are constants to be determined by the initial conditions of the system.

The behavior of the solution, equation (3.27), depends on solutions s_1 and s_2. Considering only the damped case ($\zeta \neq 0$), there are three cases:

a) underdamped system ($\zeta < 1$): it results in a harmonic motion with a exponentially decaying amplitude. It is the only case with oscillatory motion;
b) critically damped system ($\zeta = 0$): in this case, both solutions are equal ($s_1 = s_2$). The movement is non periodic and the displacement tends to the neutral position over a large enough period of time. It is also the fastest to reach a resting state;
c) overdamped system ($\zeta > 1$): as in the previous case, the movement is non periodic and exponentially decaying.

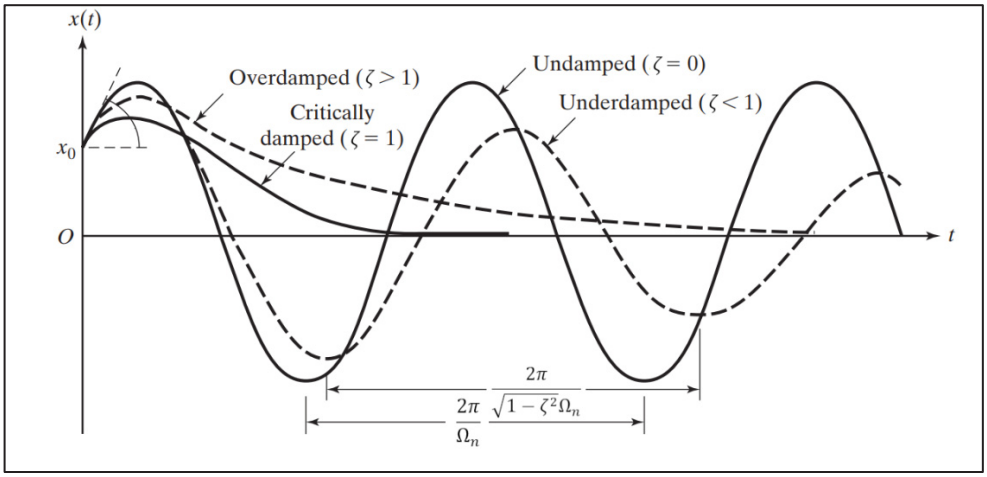

Figure 3.3 – Comparison of motions with different types of damping. Source: adapted from Rao (2004).

This is so, assuming the solution for the homogenous part of the ODE $x(t) = Xe^{i\Omega t}$ and the excitation in the form $f(t) = Fe^{i\Omega t}$. It is important to note that both X and F are complex in order to include the amplitude and phase information of the signals. Substituting it into (3.21), the problem now becomes

$$(-m\Omega^2 + i\Omega c + k)X = F \tag{3.28}$$

By definition, the frequency-response function is a transfer function - that is the ratio between the input and output signals in the frequency domain -, which leads to

$$\alpha(\Omega) = \frac{X}{F} = \frac{1}{-m\Omega^2 + i\Omega c + k} \tag{3.29}$$

This particular FRF is known as *Receptance* and uses the displacement as a response parameter. This ratio is complex as there is both an amplitude ratio and phase angle between the two sinusoids.

If, instead of displacement, velocity is used as the input parameter, a different FRF is obtained, known as *Mobility*. Considering that displacement and velocity are mathematically relatable, this relation can be used to obtain the following mobility equation:

$$v(t) = \dot{x}(t) = Ve^{i\Omega t} = i\Omega Xe^{i\Omega t} \tag{3.30}$$

which leads to

$$Y(\Omega) = \frac{V}{F} = \frac{i\Omega}{-m\Omega^2 + i\Omega c + k} = i\Omega\, \alpha(\Omega) \tag{3.31}$$

The same process can be used to obtain the FRF Inertance, which uses acceleration as the response parameter, and so

$$a(t) = x(t) = Ae^{i\Omega t} = -\Omega^2 Xe^{i\Omega t} \tag{3.32}$$

$$I(\Omega) = \frac{A}{F} = -\frac{\Omega^2}{-m\Omega^2 + i\Omega c + k} = -\Omega^2\, \alpha(\Omega) \tag{3.33}$$

Those are the main formulations of FRF's. However, there are still the inverse formulations that, although not commonly used, have a purpose in the present project.

Table 3.1 – Definition of Frequency Response Functions

Response parameter R	**Standard FRF: R/F**	**Formulation**	**Unit**	**Inverse FRF: F/R**	**Formulation**	**Unit**
Displacement	Receptance	$\frac{X}{F}$	$\frac{m}{N}$	Dynamic Stiffness	$\frac{F}{X}$	$\frac{N}{m}$
Velocity	Mobility	$\frac{V}{F}$	$\frac{m}{Ns}$	Mechanical Impedance	$\frac{F}{V}$	$\frac{Ns}{m}$
Acceleration	Inertance	$\frac{A}{F}$	$\frac{m}{Ns^2}$	Dynamic Mass	$\frac{F}{A}$	$\frac{Ns^2}{m}$

Previously, the response functions were defined as a ratio of the response over the impulse, or R/F. The reciprocal functions are the ratio of the impulse over the response, or F/R.

3.3. MULTIPLE-DEGREES-OF-FREEDOM SYSTEM VIBRATION

Extending the idea of the SDOF problem to an N-degrees-of-freedom problem, several equations of motion are obtained - one for each degree of freedom - that can be written in matrix form as follows:

$$[M]\{\ddot{x}(t)\} + [C]\{\dot{x}(t)\} + [K]\{x(t)\} = \{f(t)\} \quad (3.34)$$

where $[M]$, $[C]$ and $[K]$ are *N x N* mass, damping, and stiffness matrices, respectively, and $\{x(t)\}$ and $\{f(t)\}$ are *N x 1* vectors of time-varying displacement and forces. As in the previous section, more detailed explanation can be found in Ewins (1984).

3.3.1. Undamped multiple-degrees-of-freedom systems

Every real system presents a certain level of damping, so the analysis of undamped systems does not perfectly represent reality; however, it leads to important conclusions that will be used in later analysis.

Assuming the answer takes the form of $\{x(t)\} = \{X\}e^{i\Omega t}$, and the system is in free vibration mode - in other words, $f = 0$ -, the system can be simplified to

$$(-\Omega^2[M] + [K])\{X\}e^{i\Omega t} = 0 \quad (3.35)$$

the only non-trivial solutions for it are those that satisfy (3.36)

$$\det(-\Omega^2[M] + [K]) = 0 \quad (3.36)$$

from which *N* values for Ω^2 can be found, the undamped natural frequencies of the system. Substituting those back into (3.35), the result will be a solution ψ_r of X, known as eigenvector. With Ω_r being the natural frequency (in *rad/s*) of mode *r*, and the eigenvector ψ_r the corresponding mode shape, by ordering the eigenvalues such as $\Omega_1^2 \leq \Omega_2^2 \leq \Omega_3^2 \leq \cdots \leq \Omega_n^2$, the modal matrix can be constructed such that $\Psi = [\psi_1\ \psi_2 \ldots \psi_n]$. The eigenvalues can also be arranged in matrix form by making the values the diagonal of the matrix

$$[\Lambda] = \begin{bmatrix} \ddots & & \\ & \Omega_r^2 & \\ & & \ddots \end{bmatrix} \quad (3.37)$$

It is important to note that the eigenvalue matrix is unique, whereas the eigenvectors matrix is not. Each eigenvector is subject to a random scaling vector that affects its magnitude, but not its shape.

$$\begin{Bmatrix} 1 \\ -1 \\ 3 \end{Bmatrix} \text{ represents the same shape as } \begin{Bmatrix} 2 \\ -2 \\ 6 \end{Bmatrix}$$

What determines how the eigenvectors are scaled depends on the numerical procedure used to obtain them. In order to eliminate the problems that arise from this

arbitrary scaling, a normalization process is performed, which takes advantage of the orthogonality properties of the modal matrices. That means that the following relations are true:

$$[\Psi]^T[M][\Psi] = [m_r] \tag{3.38}$$

$$[\Psi]^T[K][\Psi] = [k_r] \tag{3.39}$$

$$[\Lambda] = [m_r]^{-1}[k_r] \tag{3.40}$$

both $[m_r]$ and $[k_r]$ are diagonal matrices, where each m_r and k_r are the modal mass and modal stiffness of mode *r*. While m_r and k_r are subject to the arbitrary scaling, the relation $\Omega_r^2 = k_r/m_r$ is unique. The usual process for modal analysis is the mass normalization, and so, the relation between the mass normalized vector $\phi_r$and its general form ψ_r is given by

$$\{\phi\}_r = \frac{1}{\sqrt{m_r}}\{\psi\}_r \tag{3.41}$$

The mass-normalized eigenvector matrix is written as Φ and is given by

$$[\Phi]^T[M][\Phi] = [I] \tag{3.42}$$

$$[\Phi]^T[K][\Phi] = [\Lambda] \tag{3.43}$$

In order to determine its response characteristics, it will be assumed that the structure is undamped, excited by a sinusoidal set of forces in the form of $\{f(t)\} = \{F\}e^{i\Omega t}$, and that a solution exists in the form of $\{x(t)\} = \{X\}e^{i\Omega t}$. The equation of motion then becomes

$$(-\Omega^2[M] + [K])\{X\}e^{i\Omega t} = \{F\}e^{i\Omega t} \tag{3.44}$$

or, rearranging it to solve for the unknown responses,

$$\{X\} = (-\Omega^2[M] + [K])^{-1}\{F\} \tag{3.45}$$

$$\{X\} = [\alpha(\Omega)]\{F\} \tag{3.46}$$

where $[\alpha(\Omega)]$ is the N x N receptance frequency response function (FRF) matrix for the system. The general element in the receptance FRF matrix, $\alpha_{jk}(\Omega)$, is given by

$$\alpha_{jk}(\Omega) = \left(\frac{X_j}{F_k}\right);\ F_m = 0;\ \forall m \neq k \tag{3.47}$$

Solving (3.46) for $[\alpha(\Omega)]$ would involve inversion of a system matrix at each frequency. This is very inefficient and very costly for large systems. Ewins (1984) further

develops the system in order to use modal parameters rather than spatial parameters, such as in

$$(-\Omega^2[M] + [K]) = [\alpha(\Omega)]^{-1} \tag{3.48}$$

premultiplying both sides by $[\Phi]^T$ and postmultiplying by $[\Phi]$, yielding

$$[\Phi]^T(-\Omega^2[M] + [K])[\Phi] = [\Phi]^T[\alpha(\Omega)]^{-1}[\Phi] \tag{3.49}$$

Using linear algebra properties and relations, this will eventually lead to

$$\alpha_{jk} = X_j/F_k = \sum_{r=1}^{N} \frac{(\phi_{jr})(\phi_{kr})}{\Omega_r^2 - \Omega^2} \tag{3.50}$$

It is important to note that equation (3.50) is valid only if the modes are mass-normalized. In case this is not true, the modal mass is taken into consideration, resulting in

$$\alpha_{jk} = X_j/F_k = \sum_{r=1}^{N} \frac{(\psi_{jr})(\psi_{kr})}{m_r(\Omega_r^2 - \Omega^2)} \tag{3.51}$$

where ψ_{jk} is an element of the non-normalized matrix.

A more comprehensive mathematical proof can be found in Ewins (1984), p. 60.

3.3.2. Multiple-degrees-of-freedom systems with proportional damping

A simple form to include damping in the structure is the inclusion of proportional damping. In this case, the damping matrix $[C]$ is proportional to the mass and stiffness matrices, given by

$$[C] = \beta[K] + \gamma[M] \tag{3.52}$$

It is clear that the orthogonality properties presented in section 3.3.1 still apply, and so

$$[\Psi]^T[C][\Psi] = \beta[k_r] + \gamma[m_r] = [c_r] \tag{3.53}$$

Returning to equation (3.30) and, for the case of no excitation, premultiplying by the eigenvector $[\Psi]$ and performing the coordinate change to $\{X\} = [\Psi]\{P\}$ results in

$$[m_r]\{\ddot{P}\} + [c_r]\{\dot{P}\} + [k_r]\{P\} = \{0\} \tag{3.54}$$

Since $[m_r]$, $[c_r]$ and $[k_r]$ are all uncoupled (diagonal), each r^{th} individual equation can be written as

$$m_r\ddot{p}_r + c_r\dot{p}_r + k_r p_r = 0 \tag{3.55}$$

This equation is mathematically equal to that of the single-degree-of-freedom case, and each represents a single mode of the system. It has equivalent relations to those of the SDOF case:

$$\Omega_r' = \Omega_r\sqrt{1-\zeta_r^2} \tag{3.56}$$

$$\Omega_r^2 = k_r/m_r \tag{3.57}$$

$$\zeta_r = \frac{c_r}{2\sqrt{k_r m_r}} \tag{3.58}$$

These relations are also true for the forced response analysis. In this case the receptance matrix is defined by

$$[\alpha(\Omega)] = \left[-\Omega^2 M + i\,\Omega\, C + K\right]^{-1} \tag{3.59}$$

Every individual element is given by

$$\alpha_{jk}(\Omega) = \sum_{r=1}^{N} \frac{(\psi_{jr})(\psi_{kr})}{\left(-\Omega^2 m_r + k_r\right) + i(\Omega\, c_r)} \tag{3.60}$$

By putting m_r in evidence in the denominator, it is possible to use the mass-normalized modes

$$\alpha_{jk}(\Omega) = \sum_{r=1}^{N} \frac{(\phi_{jr})(\phi_{kr})}{\left(-\Omega^2 + \Omega_r^2 + 2i\zeta_r\ \Omega\ \Omega_r\right)} \tag{3.61}$$

In the undamped model, the response tends to infinity when the frequency approaches one of the resonance frequencies. However, this model does not present this, given the imaginary part of the denominator, and thus better represents the real behavior of the structure.

3.4. THE STOCHASTIC SUBSPACE IDENTIFICATION ALGORITHM FOR OPERATIONAL MODAL ANALYSIS

The OMA theory borrows heavily from control theories, and even more so the stochastic subspace identification method (SSI). Traditionally, modal analysis is thought in continuous time. Stochastic subspace identification, however, uses discrete time formulations. Considering the stochastic response from a system as a function of time

$$\boldsymbol{x}(t) = \begin{Bmatrix} x_1(t) \\ x_2(t) \\ \vdots \\ x_M(t) \end{Bmatrix} \tag{3.62}$$

It is also important to define the space state format for the problem. Taking the general MDOF equation of motion (equation (3.34)), variable $\boldsymbol{u}(t)$ is defined as

$$\boldsymbol{u}(t) = \begin{Bmatrix} \dot{\boldsymbol{x}}(t) \\ \boldsymbol{x}(t) \end{Bmatrix} \tag{3.63}$$

Rearranging equation (3.34) to accommodate $\boldsymbol{u}(t)$, yields

$$\begin{aligned} \dot{\boldsymbol{u}}(t) &= \boldsymbol{A}\boldsymbol{u}(t) + \boldsymbol{B}\boldsymbol{x}(t) \\ \boldsymbol{x}(t) &= \boldsymbol{P}\boldsymbol{u}(t) \end{aligned} \tag{3.64}$$

where $\boldsymbol{A}$, $\boldsymbol{B}$, and $\boldsymbol{P}$ are given by

$$\boldsymbol{A} = \begin{bmatrix} -\boldsymbol{M}^{-1}\boldsymbol{C} & -\boldsymbol{M}^{-1}\boldsymbol{C} \\ \boldsymbol{I} & [0] \end{bmatrix} \tag{3.65}$$

$$\boldsymbol{B} = \begin{bmatrix} \boldsymbol{M}^{-1} \\ [0] \end{bmatrix} \tag{3.66}$$

$$\boldsymbol{P} = [[0] \quad \boldsymbol{I}] \tag{3.67}$$

Matrix $[0]$ is a null matrix, and vector $\{0\}$ is a null vector. Since all matrices of the system are of order $\times N$, this formulation expands the new system to a $2N \times 2N$ space, but, at the same time, the problem simplifies to a set of simultaneous first-order differential equations. Matrix $\boldsymbol{P}$ is called the 'observation matrix' since it includes the last N elements of the state vector $\boldsymbol{u}(t)$.

Any free decay $\boldsymbol{x}(k)$ in discrete time $t_k = k\,\Delta\,t$, where $\Delta\,t$ is the sampling time step, can be expressed as

$$\boldsymbol{x}(k) = \boldsymbol{P}\boldsymbol{D}^k\boldsymbol{u}_0 \tag{3.68}$$

where $\boldsymbol{u}_0 = \boldsymbol{u}(0)$ and $\boldsymbol{D}$ is the discrete time matrix, which is calculated by

$$\boldsymbol{D} = \exp(\boldsymbol{A}\Delta t) \tag{3.69}$$

It is important to note that $\boldsymbol{D}$ is the exponential function of a matrix, which is defined by its power series. This operation is explained in greater detail in Brincker and Ventura (2015).

Given the measured data $\boldsymbol{x}(k)$ from one channel, the first step of the SSI is to form the block Hankel matrix with np data points and $2s$ block rows, which is defined as

$$\boldsymbol{H} = \begin{bmatrix} \boldsymbol{x}(1) & \boldsymbol{x}(2) & \dots & \boldsymbol{x}(np-2s+1) \\ \boldsymbol{x}(2) & \boldsymbol{x}(3) & \dots & \boldsymbol{x}(np-2s+2) \\ \vdots & \vdots & & \vdots \\ \boldsymbol{x}(s) & \boldsymbol{x}(s+1) & \dots & \boldsymbol{x}(np-s) \\ \boldsymbol{x}(s+1) & \boldsymbol{x}(s+2) & \dots & \boldsymbol{x}(np-s+1) \\ \boldsymbol{x}(s+2) & \boldsymbol{x}(s+3) & \dots & \boldsymbol{x}(np-s+2) \\ \vdots & \vdots & & \vdots \\ \boldsymbol{x}(2s) & \boldsymbol{x}(2s+1) & \dots & \boldsymbol{x}(np) \end{bmatrix} = \begin{bmatrix} \boldsymbol{H}_1 \\ \boldsymbol{H}_2 \end{bmatrix} \tag{3.70}$$

As indicated in equation 3.70, the matrix is split in the middle into the two block Hankel matrices $\boldsymbol{H}_1$ and $\boldsymbol{H}_2$ - each with s block rows -, $\boldsymbol{H}_1$ is the upper part - also known as *the past* - and $\boldsymbol{H}_2$ is the lower part - also known as *the future* in the SSI theory. Based on the defined block Hankel matrices, the projection matrix is defined as

$$\boldsymbol{O} = E[\boldsymbol{H}_2|\boldsymbol{H}_1] \tag{3.71}$$

This operation is the conditional expected value, or the expected value of $\boldsymbol{H}_2$ given $\boldsymbol{H}_1$. The resulting matrix $\boldsymbol{O}$ is the projection matrix. The projection can be calculated by

$$\boldsymbol{O} = \boldsymbol{T}_{21}\boldsymbol{T}_{11}^{+}\boldsymbol{H}_1 \tag{3.72}$$

where $\boldsymbol{T}_{21}$ and $\boldsymbol{T}_{11}$ are block Toeplitz matrices, and $\boldsymbol{T}_{11}^{+}$ is the pseudo-inverse of $\boldsymbol{T}_{11}$. The block Toeplitz matrices are defined as

$$\boldsymbol{T}_{21} = \boldsymbol{H}_2\boldsymbol{H}_1^T \tag{3.73}$$

$$\boldsymbol{T}_{11} = \boldsymbol{H}_1\boldsymbol{H}_1^T \tag{3.74}$$

However, this is not the normally used formulation. It is just the mathematical definition. This formulation is too time-and-memory consuming in most practical applications. The projection is obtained via QR decomposition of the transposed block Hankel matrix (equation 3.70) and taking advantage of the fact that only a part of the R factor matrix is needed for the projection. A more complete mathematical description of this procedure is presented in Van Overschee and De Moor (1996).

When the projection has been calculated and the free decays have been established in the projection matrix, it is possible to show that the projection matrix can be expressed as

$$\boldsymbol{O} = \boldsymbol{\Gamma}\boldsymbol{X} \tag{3.75}$$

where $\boldsymbol{\Gamma}$ is the observability matrix and $\boldsymbol{X}$ is a matrix of Kalman states, which are simply the initial conditions for all the columns in the matrix $\boldsymbol{O}$. The observability matrix is given by

$$\boldsymbol{\Gamma} = \begin{bmatrix} \boldsymbol{P} \\ \boldsymbol{PD} \\ \boldsymbol{PD}^2 \\ \vdots \\ \boldsymbol{PD}^{s-1} \end{bmatrix} \tag{3.76}$$

If matrix $\boldsymbol{\Gamma}$ were known, the Kalman states $\boldsymbol{X}$ could be determined directly from equation 3.75. By performing a singular value decomposition on the projection matrix, $\boldsymbol{\Gamma}$ and $\boldsymbol{X}$ can be estimated by the factors of the SVD

$$\boldsymbol{O} = \boldsymbol{USV}^T \tag{3.77}$$

and then defining the estimates as

$$\hat{\boldsymbol{\Gamma}} = \mathbf{U}\mathbf{S}^{1/2} \tag{3.78}$$

$$\hat{\boldsymbol{X}} = \boldsymbol{S}^{1/2}\boldsymbol{V}^{T} \tag{3.79}$$

The discrete time matrix $\boldsymbol{D}$ estimate can be obtained by solving a least square problem. And the observation matrix $\boldsymbol{P}$ can be found by simply taking the first block of the observability.

The eigenvalues and the eigenvectors of the estimate of the discrete time system matrix are then obtained from

$$\widehat{\boldsymbol{D}} = [\Psi'][\mu_n][\Psi']^{-1} \tag{3.80}$$

These eigenvectors are not direct estimates of the mode shapes. They are obtained by transforming the eigenvectors back to the physical coordinate

$$[\Psi] = \widehat{\boldsymbol{P}}[\Psi'] \tag{3.81}$$

The corresponding continuous eigenvalues λ_n (of the continuous time system matrix $\boldsymbol{A}$) are given by

$$\lambda_n = \frac{\ln(\mu_n)}{\Delta t} \tag{3.82}$$

The natural frequencies are given by

$$\Omega_n = |\lambda_n| \tag{3.83}$$

and the modal damping by

$$\zeta_n = \frac{Re(\lambda_n)}{|\lambda_n|} \tag{3.84}$$

3.5. GENERALIZED EQUIVALENT PARAMETERS

The control of vibrations by dynamic neutralizers can be accomplished considering viscous, hysteretic, or viscoelastic damping. The latter case is the one of interest for the present project and, given its complexity, it requires the introduction of a new concept: the ‘generalized equivalent parameters’.

The definition of generalized equivalent parameters was presented by Espíndola and Silva (1992). This definition allows the description of the compound system in function of its generalized physical coordinates of the primary system alone. This permits the analysis of a system of neutralizers attached to a primary structure, solely in terms of the modal parameters of the primary structure.

The simple neutralizer is composed of a rigid mass connected through some resilient element. It may be a spring in parallel with a shock absorber or viscoelastic material, such as a rubber, with complex stiffness

$$\bar{K}(T,\Omega) = L\bar{G}(T,\Omega) = LG_r(T,\Omega)[1 + i\eta(T,\Omega)] \tag{3.85}$$

where $\bar{K}$ is the complex stiffness, L is the geometric factor of the connecting element, $\bar{G}$ is the complex shear modulus – with G_r being its real part –, and η is the loss factor. As can be seen from equation (3.85), the complex stiffness and modulus are dependent on temperature T and frequency Ω, since the neutralizers will operate in a controlled environment, with constant temperature. For the sake of simplicity, the T will be omitted from following equations.

In Figure 3.4, $X_b(\Omega)$ and $F(\Omega)$ are the Fourier transforms of the displacement $x_b(t)$ and force $f(t)$ applied to the base, respectively. Also, the mass of the base is considered negligible.

By performing a free body diagram analysis and using the definition of a transfer function, both the mechanical impedance and dynamic mass at the base can be obtained, they are, respectively

$$Z_a(\Omega) = \frac{F(\Omega)}{V(\Omega)} = -im_a\Omega\frac{im_a\Omega\, L\bar{G}(\Omega)}{m_a\Omega^2 - L\bar{G}(\Omega)} \tag{3.86}$$

$$M_a(\Omega) = \frac{F(\Omega)}{A(\Omega)} = -m_a\frac{L\bar{G}(\Omega)}{m_a\Omega^2 - L\bar{G}(\Omega)} \tag{3.87}$$

where $V(\Omega) = i\Omega X_b(\Omega)$ and $A(\Omega) = -\Omega^2 X_b(\Omega)$ are the velocity and the acceleration in the frequency domain, respectively, and m_a is the mass of the neutralizer.

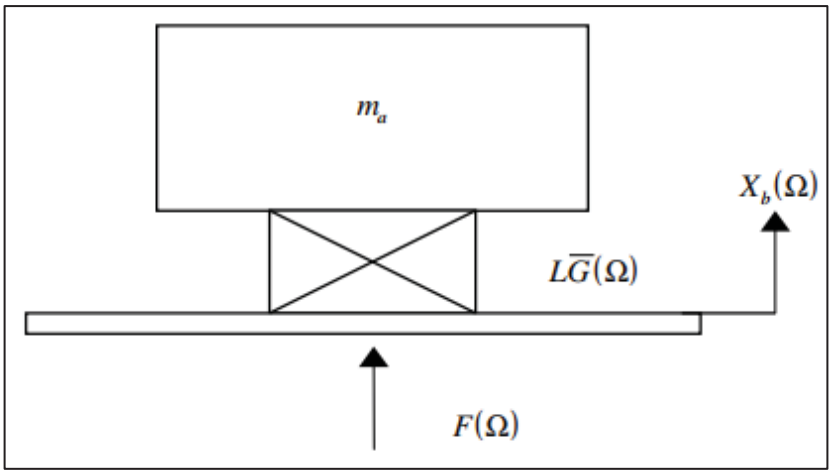

Figure 3.4 – Representation of a SDOF neutralizer. Source: adapted from Bavastri (1997).

The antiresonance frequency of the neutralizer is defined in such a way that, in the absence of damping, the denominator of the equations (3.86) and (3.87) is equal to zero,

$$\Omega_a^2 = \frac{L\bar{G}(\Omega)}{m_a} \tag{3.88}$$

When the natural frequency of the structure approaches the antiresonance frequency, both the mechanical impedance and dynamic mass approach its maximum value. This means that an infinite force is necessary for a finite displacement. This is the fundamental working principle of vibration neutralizers.

Equations (3.86) and (3.87) can be simplified by defining $r(\Omega) = G_r(\Omega)/G_r(\Omega_a)$ and $\varepsilon_a = \Omega / \Omega_a$,

$$Z_a(\Omega) = -im_a\Omega \frac{r(\Omega)\,[1 + i\eta(\Omega)]}{\varepsilon_a^2 - r(\Omega)\,[1 + i\eta(\Omega)]} \tag{3.89}$$

$$M_a(\Omega) = -m_a \frac{r(\Omega)\,[1 + i\eta(\Omega)]}{\varepsilon_a^2 - r(\Omega)\,[1 + i\eta(\Omega)]} \tag{3.90}$$

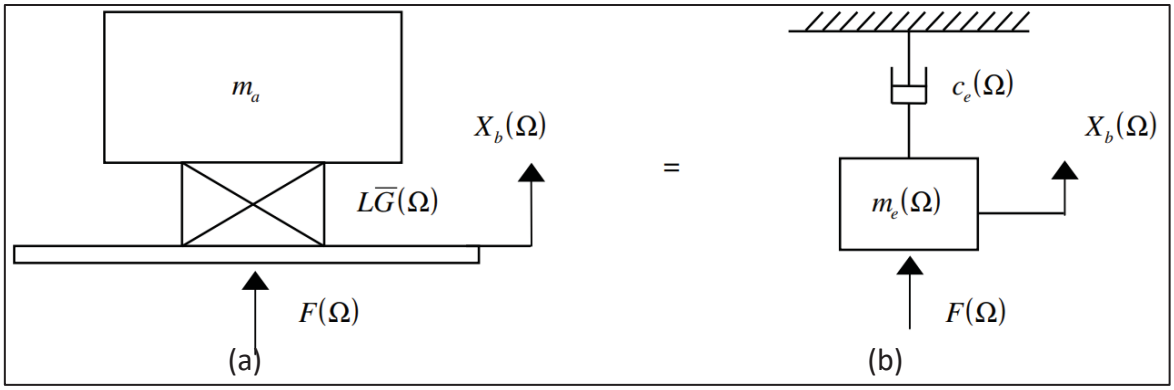

Figure 3.5 –Equivalency diagrams: (a) real neutralizer; (b) equivalent neutralizer. Source: adapted from Bavastri (1997).

Analyzing the equivalent system from Figure 3.5, and considering that $k_{eq}(\Omega) = -\Omega^2 m_{eq}(\Omega) + i\Omega c_{eq}(\Omega)$, the mechanical impedance and the dynamic mass are, respectively,

$$Z_a(\Omega) = \frac{F(\Omega)}{i\Omega X_b(\Omega)} = i\Omega m_{eq}(\Omega) + c_{eq}(\Omega) \tag{3.91}$$

and

$$M_a(\Omega) = \frac{F(\Omega)}{-\Omega^2 X_b(\Omega)} = m_{eq}(\Omega) - \frac{ic_{eq}(\Omega)}{\Omega} \tag{3.92}$$

Comparing equations (3.87) and (3.88) to equations (3.85) and (3.86), it is clear that

$$m_{eq}(\Omega) = \text{Real}\big(M_a(\Omega)\big) = -m_a \frac{r(\Omega)\,\{\varepsilon_a^2 - r(\Omega)\,[1+\eta^2(\Omega)]\}}{[\varepsilon_a^2 - r(\Omega)]^2 + [r(\Omega)\,\eta(\Omega)]^2} \tag{3.93}$$

and

$$c_{eq}(\Omega) = \text{Real}\big(Z_a(\Omega)\big) = m_a\Omega_a \frac{r(\Omega)\,\eta(\Omega)\varepsilon_a^3}{[\varepsilon_a^2 - r(\Omega)]^2 + [r(\Omega)\,\eta(\Omega)]^2} \tag{3.94}$$

This equivalency (Figure 3.5) shows that the primary system responds to the neutralizer as a mass $m_{eq}(\Omega)$ and a viscous damper $c_{eq}(\Omega)$ grounded and attached in series along a generalized coordinate $x_b(t)$.

The importance of the equivalent system is that the dynamics of the compound system can be formulated in function of the physical coordinates of the primary system alone, even though the system has now additional degrees of freedom.

3.6. PRIMARY COORDINATES AND RESPONSE FUNCTION OF SIMPLE DYNAMIC VISCOELASTIC NEUTRALIZERS

The equations of motion in their matrix form (3.34) can be rewritten, without any loss of generality, in the frequency domain through the Fourier transform. So, the equation becomes

$$(-\Omega^2[M] + i\Omega[C] + [K])X(\Omega) = F(\Omega) \tag{3.95}$$

with $X(\Omega)$ and $F(\Omega)$ are the fourier transforms for $x(t)$ and $f(t)$, respectively.

The next step is to perform the transformation of coordinates

$$X(\Omega) = \Phi P(\Omega) \tag{3.96}$$

where $X(\Omega)$ are the physical coordinates of the problem, also known as the 'generalized coordinates'; and $P(\Omega)$ is known as the 'primary coordinates'. Pre-multiplying equation (3.95) by Φ gives

$$(-\Omega^2\, I + i\Omega\, \Phi^T C\Phi + \Lambda)P(\Omega) = \Phi^T F(\Omega) = N(\Omega) \tag{3.97}$$

It is important to note that

$$\Phi^T C\Phi = \begin{bmatrix} \ddots & & \\ & 2\xi_r\Omega_r & \\ & & \ddots \end{bmatrix} \tag{3.98}$$

where ξ_r and Ω_r are the damping ratio and the resonance frequency of the r-th mode, respectively.

This coordinate transform turns the problem into a modal space one. The main feature of this space is that the system of equations is uncoupled. In other words, elements outside the main diagonal are zero. The practical effect of this uncoupling is that each equation r can be solved independently.

When the neutralizers are attached to the structure, using generalized equivalent parameters, $[M]$ and $[C]$ can be substituted by $\left[\widetilde{M}\right]$ and $\left[\tilde{C}\right]$ in equation (3.95), where

$$\left[\widetilde{M}\right] = [M] + \begin{bmatrix} \ddots & & 0 \\ & m_{eq,p}(\Omega) & \\ 0 & & \ddots \end{bmatrix} = [M] + \left[M_{eq}\right] \tag{3.99}$$

and

$$\left[\tilde{C}\right] = [C] + \begin{bmatrix} \ddots & & 0 \\ & c_{eq,p}(\Omega) & \\ 0 & & \ddots \end{bmatrix} = [C] + \left[C_{eq}\right] \tag{3.100}$$

Following the same steps as before

$$\left(-\Omega^2[\, I + \Phi^T M_{eq}\Phi] + i\Omega\left[\Phi^T C\Phi + \Phi^T C_{eq}\Phi\right] + \Lambda\right)P(\Omega) = N(\Omega) \tag{3.101}$$

In order to simplify, variable D is introduced, defined by $[D] = \left(-\Omega^2[\, I + \Phi^T M_{eq}\Phi] + i\Omega\left[\Phi^T C\Phi + \Phi^T C_{eq}\Phi\right] + \Lambda\right)$, so the system from equation (3.96) becomes

$$[D]P(\Omega) = N(\Omega) \tag{3.102}$$

Returning to the physical space and rearranging equation (3.91), it becomes

$$X(\Omega) = \Phi[D]^{-1}\Phi^T F(\Omega) \tag{3.103}$$

By definition, the transfer function is given by X/F – equivalent to equation (3.50) from the SDOF case.

$$\alpha(\Omega) = \Phi[D]^{-1}\Phi^T \tag{3.104}$$

where $\alpha(\Omega)$ is the $n\ x\ n$ receptance matrix. Given the orthogonal properties of the modal matrix, $\alpha(\Omega)$ is symmetrical. This is known as the 'reciprocity principle', discussed in chapter 3.3. The individual elements of the receptance matrix can be calculated by

$$\alpha_{ks}(\Omega) = \sum_{j=1}^{n}\sum_{i=1}^{n} D_{ij}^{-1}\Phi_{si}\Phi_{kj} \tag{3.105}$$

With this function, it is possible to determine the response of the compound system for any given neutralizer or set of neutralizers. It is dependent only on the modal characteristics of the primary system and the generalized equivalent parameters of the neutralizers. This means that, in an iterative process such as optimization, it is not necessary

to recalculate the modal parameters of the system (eigenvalues and eigenvectors) in each iteration, making this methodology computationally very efficient.

3.6.1. Truncated modal matrix

A multiple-degrees-of-freedom system has the same number of modes as the number of degrees of freedom. In mathematical terms, that means the modal matrix is square. However, the most common practice for modal analysis is that only the modes within a certain frequency band are identified, be it by the limitations of the test setup or simply by choice. This results in a truncated matrix, where the number of modes is smaller than the number of degrees of freedom or, simply put, the modal matrix is rectangular.

As previously stated, each column of the modal matrix represents a mode shape and has an associated natural frequency to it. By limiting the frequency band for analysis, the resulting matrix has an order of $n\ x\ \hat{n}$; $\hat{n} < n$, where n is the number of degrees of freedom, and $\hat{n}$ is the number of identified modes.

Returning to equation (3.95), the same steps can be performed to define the equations for the truncated case. Starting with the coordinate transformation

$$X(\Omega) = \widehat{\Phi}\hat{P}(\Omega) \tag{3.106}$$

Then, pre-multiplying equation (3.95) by $\widehat{\Phi}^T$, the new equation is

$$\left(-\Omega^2[\,\hat{I} + \widehat{\Phi}^T M_{eq}\widehat{\Phi}] + i\Omega\left[\widehat{\Phi}^T C\widehat{\Phi} + \widehat{\Phi}^T C_{eq}\widehat{\Phi}\right] + \widehat{\Lambda}\right)\hat{P}(\Omega) = \widehat{\Phi}^{\mathrm{T}} F(\Omega) \tag{3.107}$$

Despite being very similar to the non-truncated version, the fact that the modal matrix is no longer square requires an extra attention regarding the order of the matrices.

For matrix multiplication, the order of the involved matrices must always agree. Taking for example the first term, in the previous case $\left(\Phi^T\right)_{n\,x\,n}(M)_{n\,x\,n}(\Phi)_{n\,x\,n}$, which resulted in a $n\ x\ n$ matrix. Now, this changes into $\left(\widehat{\Phi}^T\right)_{\hat{n}\,x\,n}(M)_{n\,x\,n}\left(\widehat{\Phi}\right)_{n\,x\,\hat{n}}$, which results in a $\hat{n}\ x\ \hat{n}$ matrix; keeping in mind that, when a rectangular matrix is transposed, its order is inverted, that said, not much else changes from the previous case.

Defining the variable $\left[\widehat{D}\right] = \left(-\Omega^2[\,\hat{I} + \widehat{\Phi}^T M_{eq}\widehat{\Phi}] + i\Omega\left[\widehat{\Phi}^T C\widehat{\Phi} + \widehat{\Phi}^T C_{eq}\widehat{\Phi}\right] + \widehat{\Lambda}\right)$, the receptance matrix can be written as

$$\alpha(\Omega) = \widehat{\Phi}[\widehat{D}]^{-1}\widehat{\Phi}^T \tag{3.108}$$

and each individual element is given by

$$\alpha_{ks}(\Omega) = \sum_{j=1}^{\hat{n}} \sum_{i=1}^{\hat{n}} \widehat{D}_{ij}^{-1} \widehat{\Phi}_{si} \widehat{\Phi}_{kj} \tag{3.109}$$

3.7. NONLINEAR OPTIMIZATION TECHNIQUES

Optimization is the field of mathematics dedicated to finding the minimum (or maximum) of a function. In engineering design, it is the process of finding the best possible design. As stated by Arora (2016), the main difference between a conventional design process and an optimum design process is that, in the conventional process, the changes to the design are based on experience, and the final design is set when performance is satisfactory. In the optimization process, the trial design is analyzed to determine if it is the best possible design.

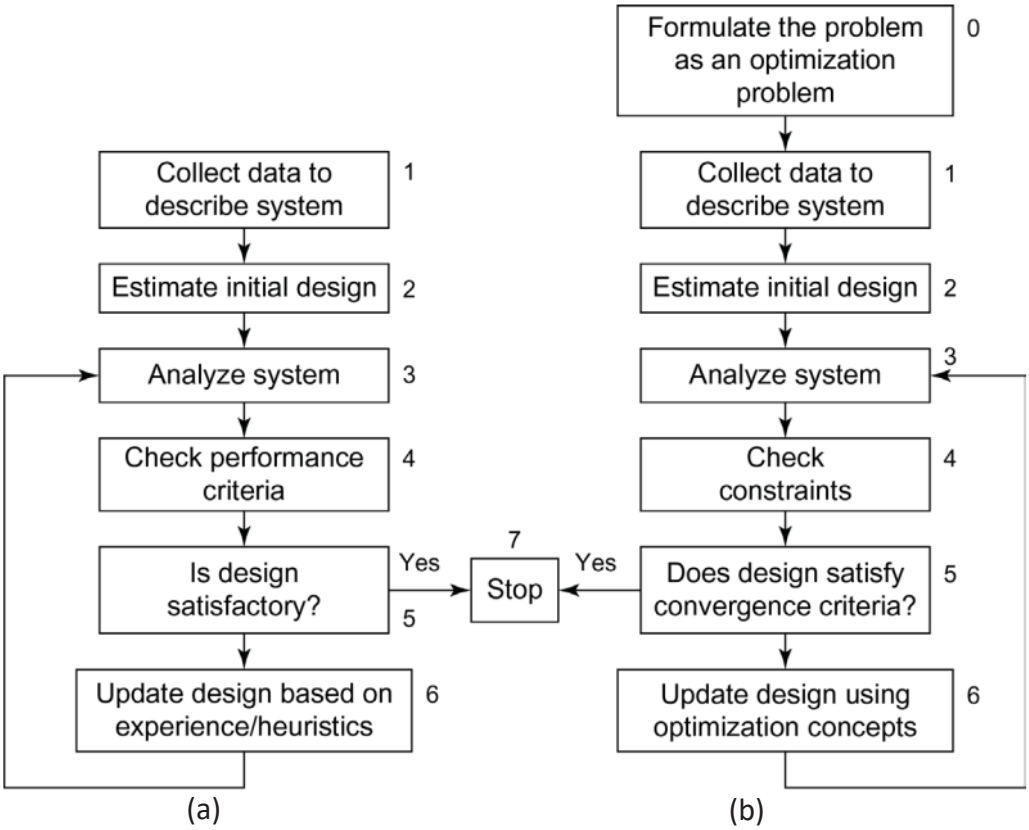

Figure 3.6 – Comparison of (a) a conventional design with (b) an optimum design. Source: Arora (2016).

The objective of an optimization problem is to find the optimal point of an objective function in its design space $\mathbb{R}^n$ (n dimensions), subjected or not to constraints. Mathematically, the problem is presented in the standard form

$$
\begin{aligned}
&minimize\ f(\boldsymbol{x}) \qquad && f: \mathbb{R}^n \to \mathbb{R} \\
& && \boldsymbol{x} \in \mathbb{R}^n \\
&subject\ to: && \\
&h_i(\boldsymbol{x}) = 0 && i = 1, 2, 3, \dots, m \\
&g_j(\boldsymbol{x}) \geq 0 && j = 1, 2, 3, \dots, n
\end{aligned}
\tag{3.110}
$$

Function $f(\boldsymbol{x})$ is called the 'objective function'. It is the function to be optimized and it maps an n-dimensional space to a scalar (1D space). The equality constraints are given by $h_i(\boldsymbol{x})$, all of which must be written in such way that they are equal to zero. And the inequality constraints are given by $g_j(\boldsymbol{x})$, and they should be such that they are all greater than or equal to zero. The design parameters vector is given by $\boldsymbol{x}$. The region where $\boldsymbol{x}$ satisfies all constraints is called the 'feasible region', otherwise it is known as the 'infeasible region'.

The problem can be linear or nonlinear. It is linear if the objective function and the constraint functions are all polynomial of degree zero or one. Otherwise it is nonlinear, and that represents most of engineering problems.

In Arora (2016), the search methods for nonlinear optimization can be classified as Derivative-Based Methods, Derivative-Free Methods, Direct Search Methods, and Nature Inspired Methods.

The Derivative-Based Methods are iterative methods that use the first-order derivative information of the function (gradient), and some use even the second-order information (Hessian matrix) about the problem, known as 'Newton methods'. And those that use approximate second-order information using only first-order information are known as 'quasi-Newton methods'. In practice, a numerical method may take a large number of iterations to reach an optimum point. Therefore, it is important to employ methods having a faster convergence, and the first- and second-order information help increase the overall convergence rate. However, this class requires that all functions of the problem be continuous - at least up to its second-order derivatives they are also continuous -; accurate first-order derivatives of all functions be available, and design variables be also continuous within their allowed range.

Derivative-Free Methods do not require the explicit calculation of the analytical derivatives of the functions. Instead, an approximation of derivatives is used to construct a local model. The functions are, again, assumed to be continuous and differentiable.

Approximation to the derivatives is generated using solely the function values, such as in the finite difference approach. This class also includes the response surface methods that generate approximation for complex optimization functions using solely the function values and regression analysis.

Unlike the two previous methods, the Direct Search Methods do not depend on the analytical or approximate derivatives of the functions. This means that the methods can be used for problems where the derivatives are expensive to calculate or are unavailable due to lack of differentiability of functions. The functions are still assumed to be continuous and differentiable.

Nature inspired search methods have its origins in natural phenomena, like evolution or moving pattern of ants. In contrast to the other direct search methods, nature inspired methods do not require the continuity or differentiability of problem functions. The only requirement is to be able to evaluate functions at any point within the allowable ranges for the design variables. They use stochastic ideas and random numbers in their calculations and decisions made at most steps of the algorithms and, by the fact they are executed at different times, the algorithms can lead to a different sequence of designs and a different solution even with the same initial conditions.

According to Arora (2016), once an optimization problem has been formulated, a suitable method needs to be selected to solve the problem. For that, answering the following questions might help in selecting the method:

a) are the design variables continuous, discrete, or integer?
b) are the problem functions continuous and differentiable?
c) are derivatives of all the problem functions available (can be calculated efficiently)?

For the proposed problem, the design variables are continuous, the functions are continuous and assumed to be differentiable, and the derivatives cannot be efficiently calculated for all functions (particularly the objective function). Based on that, a direct search method was chosen, more specifically the Nelder-Mead simplex algorithm.

3.7.1. Nelder-Mead simplex method

This method uses the idea of a simplex, which is a geometric figure formed by a set of $n + 1$ points in the *n*-dimensional space (noting that *n* is the number of design variables), developed in Nelder and Mead (1965). When the points are equidistant, the simplex is said to be regular. In two dimensions, the simplex is just a triangle; in three dimensions, it is a tetrahedron, and so on.

The basic idea of the Nelder–Mead method is to compute the objective function value at the $n + 1$ vertices of the simplex and move this simplex towards the minimum point. The algorithm accomplishes this by performing four operations on the simplex: *reflection*, *expansion*, *contraction,* and *shrinking*. At each iteration, the vertex with the largest cost function value is replaced with another vertex with a better cost function value. The algorithm can be used for general constrained optimization problems by converting the problem into an unconstrained one by replacing the original objective function by a penalized function.

3.7.1.1. Termination criteria

A termination criterion is needed to stop the iterative process of the Nelder–Mead algorithm. The criteria are:

a) the domain convergence test: When the simplex is sufficiently small. This is evaluated by comparing if the distance of the best point $\boldsymbol{x}^{(1)}$ to all others are within a tolerance, $\left|\boldsymbol{x}^{(1)} - \boldsymbol{x}^{(j)}\right| < 10^{-6},\ j = 2, 3, \dots, n + 1$;

b) the function value convergence test: When the function values variation is sufficiently small. This is evaluated by comparing the difference between the function value of the best point with all others, $\left|f\left(\boldsymbol{x}^{(1)}\right) - f\left(\boldsymbol{x}^{(j)}\right)\right| < 10^{-6},\ j = 2, 3, \dots, n + 1$;

c) the limit on number of iterations: When the limit on number of iterations exceeds a specified value, $i \geq 200$.

The algorithm is terminated if *a* and *b* are simultaneously satisfied, or *c* is satisfied.

3.7.2. Penalty function method

Some minimization methods can only be used for unconstrained problems, including the Nelder-Mead algorithm. However, it is possible to modify a constrained minimization problem into an unconstrained problem. The most notable methods are the penalty function method, the barrier function method, and the augmented Lagrangian multiplier. The first is the one used in the present work.

Defining a function

$$f^*(\boldsymbol{x}, r) = f(\boldsymbol{x}) + P\big(h_i(\boldsymbol{x}), g_j(\boldsymbol{x}), r\big) \tag{3.111}$$

where $f^*(\boldsymbol{x}, r)$ is the modified unconstrained objective function, $f(\boldsymbol{x})$ is the original function subject to constraints, $P\big(h_i(\boldsymbol{x}), g_j(\boldsymbol{x}), r\big)$ is the penalty function, and r is penalty parameter. Since the problem presented does not contain any equality constraints, the term $h_i(\boldsymbol{x})$ will be ignored.

In the penalty function method, function P is defined in such a way that, when the constraints are violated, the objective function f is penalized by adding a positive value to it, thus forcing the algorithm to return its search to the feasible region. Out of the several possible penalty functions, the most used is the quadratic loss function, which can be defined as

$$P\big(g_j(\boldsymbol{x}), r\big) = r \sum_{j=1}^{n} \big[g_j^+(\boldsymbol{x})\big]^2; \quad g_j^+(\boldsymbol{x}) = \max\Big(0, g_j(\boldsymbol{x})\Big) \tag{3.112}$$

By definition, $g_j^+(\boldsymbol{x}) \geq 0$, it is zero if the inequality is active or inactive ($g_j(\boldsymbol{x}) \leq 0$), and positive if the inequality is violated ($g_j(\boldsymbol{x}) > 0$). In practical terms, the penalty function P is only relevant when the algorithm is evaluating points outside the feasible region. Inside the feasible region, the objective function remains unchanged.

Both the linear and quadratic loss functions form a continuous modified function. The advantage of the quadratic function over the linear one is that the first derivative is also continuous for the quadratic penalty function.

The advantages and disadvantages of the penalty function are:

a) it is applicable to generally constrained problems, with equality and inequality constraints (one or both);
b) the starting point can be arbitrary, including points outside the feasible region;

c) they may iterate through the infeasible region where the objective and constraint functions can be undefined;
d) if the iterative process terminates prematurely, the final point may not be inside the feasible region and hence not usable.

Because of *d*, extra care has to be taken when analyzing the result of optimization. Normally, the result is just outside the feasible region, so it is just a matter of choosing the nearest feasible point.

4. METHODOLOGY

The first step for the development of this work was to perform experimental and operational modal analyses in order to obtain the modal parameters used as input for the algorithm. Next, the existing algorithm was adapted for the new problem and data sets.

The algorithm outputs the mass and resonance frequencies of the neutralizers; those values were used to specify the dimensions of the neutralizer, with which the neutralizers were built accordingly.

Finally, a new round of tests was performed in order to validate the methodology. The results are shown in the next chapter.

4.1. MODAL ANALYSIS

Modal analysis is the set of processes that test components or structures aiming to obtain the mathematical description of the dynamic and vibration behavior of said structures and components. The main results of a modal analysis are the modal parameters, namely the natural frequencies, mode shapes, and modal damping.

The basic principle is to excite the structure with a hammer, a shaker or even by its own operation. Then, the dynamic response is measured, most commonly the acceleration via a single accelerometer or a set of them. Given the necessary inputs and outputs, it is possible to calculate the necessary FRF's, which are the inputs for the algorithm to determine the modal parameters.

This approach is known as 'experimental modal analysis' (EMA). Alternatively, an 'operational modal analysis' (OMA) can be performed. The main difference is that, in OMA, the magnitude of the input is not known; it is assumed to be a white noise, instead. This leads to non-mass normalized mode shapes.

4.1.1. Experimental modal analysis

As mentioned, the basic principle of EMA is that the excitation and response are measured, in order to obtain the FRF's. There are several ways to excite the structure and measure its response. One of the most used methods for vibrating a structure is by using a

shaker, a device that generates an alternating motion that induces vibration upon the structure. The force is usually measured by a load cell installed at the connection point between the structure and the shaker. The three main types of excitation methods are:

a) the mechanical method: an out-of-balance rotating mass, for example, where the frequency can be controlled by adjusting the motor speed;
b) the electromagnetic method: where the device transforms an electrical signal into motion, and the frequency can be controlled via a signal generator;
c) the electrohydraulic method: the vibration is generated by hydraulic actuators, and the frequency can be controlled by changing the speed of the actuators.

Another very common method is the impact test, used in this project. This test is a relatively simple way of exciting the structure. It consists of a hammer (or hammer-like object) used to hit and excite the structure. On the tip of the hitting tip of the hammer, there is a load cell - or force transducer - that detects the magnitude felt by the impactor. This impact is assumed to be equal in magnitude and opposite in direction to that experienced by the structure. The idea here is that the impact of the hammer is short enough to approach the unitary impulse. In the frequency domain, the unitary impulse spans the whole domain. However, in actual testing conditions, this is impossible to achieve, meaning that the impact approaches a half-sine curve; and, in the frequency domain, it is flat up until a limit frequency and then it decreases, as shown in Figure 4.1.

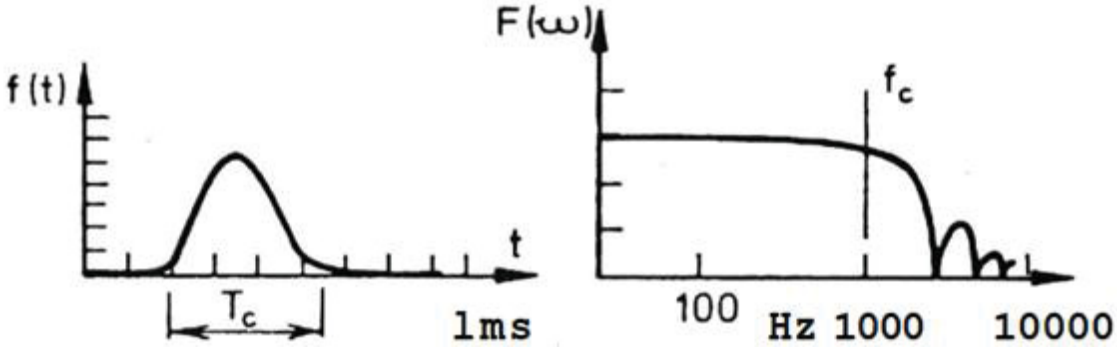

Figure 4.1 – Unitary pulse in the time and frequency domains. Source: adapted from Ewins (1984).

The test was performed by fixating an accelerometer in the structure (point 1, as shown in Figure 4.2c) and hitting the structure with the hammer at all points. Given the reciprocal property of the FRF's ($\alpha_{jk} = \alpha_{kj}$), there is no need to measure the acceleration at the other points. The analysis was performed using the Siemens LMS Test.Lab software.

4.1.2. Operational modal analysis

Operational modal analysis was developed - as the name suggests - for operating conditions of structures. It is mostly used in cases where there is no proper testing setup, and so the exciting forces cannot be properly measured. One example is the use in buildings, where the excitation is given by the movement of people inside the building, nearby traffic, and the wind. Another case concerns airplanes, where vibration is induced by its in-use conditions during a test flight. In both cases, the vibration produced has white noise characteristics. The two major disadvantages of OMA are the fact that the modal matrix is not mass-normalized, and, given the random nature of the excitation, the eventual lack of excitation of some modes.

Although it is possible to perform an OMA test by placing sensors at every measurement point of the structure, this is an unlikely situation. Instead, one or more sensors are used as reference sensors and do not change position during the test. The other sensors, called ‘roving sensors’, change their position with each run in order to cover all points.

The test was performed by hitting the structure with the hammer in a random fashion, and measuring the response at all points. The response must be measured at all points because the impact is not known, and so the reciprocal property does not apply. For this test, three reference accelerators were used, and five roving sensors to measure the remaining points, in a total of five runs. The analysis was performed in the ARTeMIS software using the stochastic subspace identification (SSI) algorithm.

4.2. DYNAMIC VISCOELASTIC NEUTRALIZER DESIGN

The design optimization function has the end goal of reducing the vibration amplitude throughout the structure, as defined by the objective function. The MATLAB script developed for this project can be used for any type of structure, as long as it has the modal parameters of the structure. The modal parameters were obtained via EMA and OMA. Other methods, such as FEM, may also be good alternatives.

The inputs are as follow:

a) modal parameters of the structure;
b) viscoelastic material properties.

The optimization parameters are:

a) number of neutralizers;
b) position of neutralizers;
c) modes to be controlled;
d) frequency range for control;
e) mass ratio μ.

Outputs:

a) mass of each neutralizer;
b) natural frequency of each neutralizer.

In order to obtain the optimal parameters, the parameters were set as:

a) 3 neutralizers;
b) at points 5, 11, and 26;
c) controlling modes 5, 6, and 7;
d) between the frequencies of 400 Hz and 800 Hz;
e) mass ratio $\mu = 0.1$.

4.2.1. Primary system

The primary system is a frame made of aluminum profile *40x40 light type I* (Figure 4.2a). It is light, strong, and easy to assemble and, given its modular nature, it is easy to replicate. The structure itself is made of two longitudinal bars, connected by two transversal bars (Figure 4.2b).

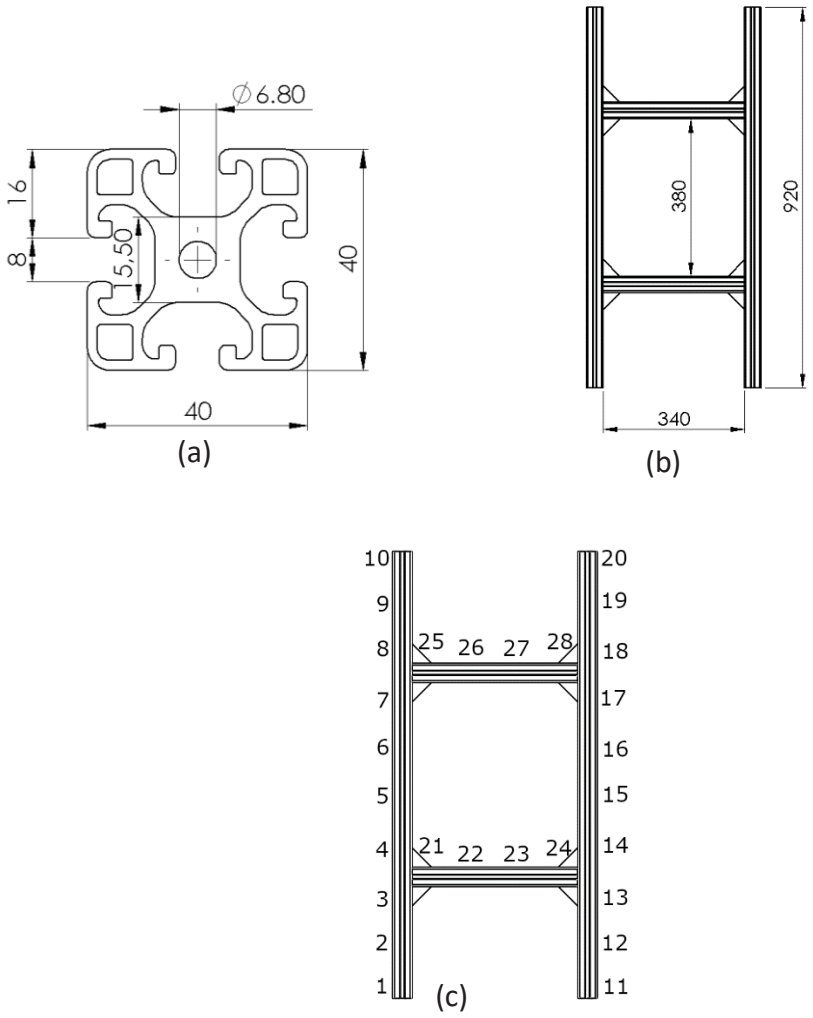

Figure 4.2 – Aluminum frame: (a) Profile; (b) Structure; (c) Numbering of points. Units in mm. Source: The Author.

For the modal analysis, the structure was divided into 28 points (Figure 4.2c), and the frequency range was between $0\ Hz$ and $1500\ Hz$, where 13 modes were identified.

4.3. DETERMINING THE MASS OF THE NEUTRALIZERS

The mass of the neutralizers (m_a) is one of the necessary parameters for the objective function. These could very easily be arbitrary values. However, Den Hartog (1956) proposed - for an SDOF system - that the mass of the neutralizer be a fraction of the mass of the primary system. For an MDOF primary system, Espídola and Silva (1992) proposed a method to determine the mass of multiple neutralizers, equivalent to Den Hartog's method.

Analyzing the modes individually, that means, disregarding the coupling from the system (3.101), individual equations can be written for each mode j, for $j = 1, 2, \dots, \hat{n}$

$$\left[-\Omega^2 \left(\widehat{m}_j + \sum_{i=1}^{p} m_{eq,i}(\Omega) \widehat{\Phi}^2_{\mathrm{rij}} \right) + i\Omega \left(\hat{c}_j + \sum_{i=1}^{p} c_{eq,i}(\Omega) \widehat{\Phi}^2_{\mathrm{rij}} \right) + \hat{k}_j \right] \hat{P}_j(\Omega) = \widehat{N}_j(\Omega) \tag{4.113}$$

Then, using the definition of transfer functions, $H_j(\Omega) = \hat{P}_j(\Omega) / \widehat{N}_j(\Omega)$ is given by:

$$H_j(\Omega) = \frac{1}{\left(\hat{k}_j - \Omega^2 \widehat{m}_j + i\Omega \hat{c}_j\right) + \sum_{i=1}^{p} \widehat{\Phi}^2_{\mathrm{rij}} \left(-\Omega^2 m_{eq,i}(\Omega) + i\Omega c_{eq,i}(\Omega) \right)} \tag{4.114}$$

The same equation, for an SDOF is:

$$H_j(\Omega) = \frac{1}{(k - \Omega^2 m + i\Omega c) + \left(-\Omega^2 m_{eq,i}(\Omega) + i\Omega c_{eq,i}(\Omega) \right)} \tag{4.115}$$

For an SDOF system, the mass ratio is given by $\mu = \frac{m_a}{M}$; where m_a is the mass of the neutralizer, and M is the mass of the primary system. Comparing equations 4.114 and 4.115, it is evident that the main difference is the term $\sum_{i=1}^{p} \widehat{\Phi}^2_{\mathrm{rij}}$, which multipllies the part of the equation that contains the information about the mass of the neutralizer (namely m_{eq} and c_{eq}). And so, for a modewise control, Espíndola and Silva (1992) proposed an equation equivalent to that of Den Hartog (1956) for MDOF systems.

$$\mu_j = \frac{\sum_{i=1}^{p} \widehat{\Phi}^2_{\mathrm{rij}} \, m_{a_i}^{(j)}}{m_j} \tag{4.116}$$

where $m_{a_i}^{(j)}$ is the mass of the i^{th} neutralizer ($i = 1, 2, \dots, p$) for thej^{th} mode ($j = 1, 2, \dots, \hat{n}$), and r_i is the position coordinate of the i^{th} neutralizer. For mass-normalized eigenvectors, m_j is equal to 1.

Castro and Bavastri (2019) expanded this idea for broadband control. Developing the system 4.116, and representing it in matrix form, 4.117 is obtained.

$$\begin{bmatrix} \left[\widehat{\Phi}^2_{r_i 1} \ \dots \ \widehat{\Phi}^2_{r_p 1}\right] & 0 \ \dots \ 0 & 0 & 0 \ \dots \ 0 \\ 0 \ \dots \ 0 & \left[\widehat{\Phi}^2_{r_i 2} \ \dots \ \widehat{\Phi}^2_{r_p 2}\right] & 0 & 0 \ \dots \ 0 \\ 0 \ \dots \ 0 & 0 \ \dots \ 0 & \dots & 0 \ \dots \ 0 \\ 0 \ \dots \ 0 & 0 \ \dots \ 0 & 0 & \left[\widehat{\Phi}^2_{r_i \hat{n}} \ \dots \ \widehat{\Phi}^2_{r_p \hat{n}}\right] \end{bmatrix} \begin{Bmatrix} m_{a_1}^{(1)} \\ \vdots \\ m_{a_p}^{(1)} \\ \hline m_{a_1}^{(2)} \\ \vdots \\ m_{a_p}^{(2)} \\ \hline \vdots \\ \hline m_{a_1}^{(\hat{n})} \\ \vdots \\ m_{a_p}^{(\hat{n})} \end{Bmatrix} = \begin{Bmatrix} \mu_1 \\ \mu_2 \\ \vdots \\ \mu_{\hat{n}} \end{Bmatrix} \tag{4.117}$$

Or simplifying to:

$$\widehat{\Phi}^2_{\hat{\mathrm{n}} \ \mathrm{x} \ \hat{\mathrm{n}}\mathrm{p}} \, M_{a_{\hat{\mathrm{n}} \ \mathrm{x} \ \hat{\mathrm{n}}\mathrm{p}}} = \mu_{\hat{n} \ x \ 1} \tag{4.118}$$

Solving the system for $\left\{m_{a_i}^{(j)}\right\}$, the answer is a vector for the masses of each neutralizer, for each mode. The mass of each neutralizer is the average of the masses of each mode.

$$m_{a_i} = \frac{\sum_{j=1}^{\hat{n}} m_{a_i}^{(j)}}{\hat{n}} \tag{4.119}$$

If there is a single neutralizer, the coefficient matrix $\widehat{\Phi}^2_{\hat{\mathrm{n}} \ \mathrm{x} \ \hat{\mathrm{n}}\mathrm{p}}$ is square, and so it has an inverse. However, if the number of neutralizers is greater than one, $\widehat{\Phi}^2_{\hat{\mathrm{n}} \ \mathrm{x} \ \hat{\mathrm{n}}\mathrm{p}}$ is not square and does not have an inverse. So, in order to solve the system, the pseudoinverse (or Moore-Penrose inverse) matrix must be used. The pseudoinverse is a matrix that can act as a partial replacement for the matrix inverse in cases where it does not exist. This matrix is frequently used to solve a system of linear equations when the system either does not have a unique solution or has many solutions.

4.4. OBJECTIVE FUNCTION

The objective of a DVN is to reduce the vibration of the primary system. When the reduction is desired in a frequency range that contains one or more resonance frequencies, it is denominated a broad band vibration control. The objective function should be defined so that, at the optimal point, the response of the system is the minimal possible, within the desired frequency range.

Several objective functions can be formulated, one of them uses the maximum value of the frequency response α_{ij}.

$$f(x) = \max_{\Omega_l \leq \Omega \leq \Omega_u} \left|\alpha_{ij}(\Omega, x)\right| \tag{4.120}$$

Where $\alpha_{ij}(\Omega, x)$ is the receptance of the compound system, measured in point i when excited in point j, given by equation (3.105). Since the receptance is in the complex domain, the maximum is taken from modulus (absolute value) of the response function. Variable x is the project vector, which has the construction parameters of the neutralizers. The maximum of the function is taken in a frequency interval that should include the chosen modes for control.

This function only takes into consideration the response and excitation points; it is a very specific case that does not always reduce the vibration in the entire structure. However, it is very useful when vibration reduction is wanted at a single point, for example, at a fixation point.

Advantages:

a) it is easy to implement;
b) it produces good results, especially when only a particular configuration of impulse and response is of interest;
c) it allows to control modes individually;
d) it does not need derivative information.

Disadvantages:

a) the function constructed in this way may exhibit non-smooth variations within the frequency interval. This will not allow the use of optimization techniques that require derivative information that would significantly accelerate the optimization process;
b) the choice of points i and j of the objective function is fundamental to reduce vibrations within the frequency range of interest. It may occur that one of these points coincides with a node, in which case this mode will not be controlled.

A variation of this objective function uses an entire row (or column) of the frequency response matrix. This results in a global control over the chosen control band and lies between this and the next case.

Another possible function is the Euclidean norm of the primary coordinates P; the reason being that P is a vector, but the result of the objective function must be a scalar in order to be optimized.

$$f(x) = \left\| \max_{\Omega_l \leq \Omega \leq \Omega_u} |P(\Omega, x)| \right\| \tag{4.121}$$

This formulation is more general than the one presented before as P is the vector that contains the displacement information of the entire structure and not a single point as in the previous case.

The Euclidean norm is a scalar that is defined as the square root of the inner product of the vector and itself. For a complex space, the norm is given by:

$$\|x\| = \sqrt{x^* \cdot x} \tag{4.122}$$

Where x is a vector, and x^* is the conjugate transpose of said vector.

Advantages:

a) since vector P contains information from the whole structure, the result is not dependent on the choice of points i and j;
b) the control is global within the frequency range.

Disadvantages:

a) the computational time will increase as the number of elements in the vector increases. This happens if the model originates from an FEM, or the modal analysis simply has too many points.

One of the properties of the modal space is that its system of equations is decoupled. However, after introducing the neutralizers, the system no longer is decoupled. That means any of the proposed objective functions may have more than one minimum.

Ultimately, the second objective function was chosen, since the control is wanted throughout the whole structure, and the system is not large.

5. ANALYSIS OF RESULTS

With the results of the experimental modal analysis and the parameters of the neutralizers defined, it is possible to design the DVN's and calculate an expected response for the modified structure.

Section 4.2 presents the inputs and outputs of the algorithm. It is important to note that the outputs are only the mass and the natural frequency of the neutralizers. In order to finalize the design, the theory presented in 3.1.1 is used.

5.1. RESULTS OF THE MODAL ANALYSIS

The analyses produced the following natural frequencies and damping ratios (Table 5.1). The first and last modes were not identified by OMA, but since they are far away from the frequency of interest, that is not a problem. It can be seen that the results are very similar, indicating that both data sets should provide similar results.

Table 5.1 – Natural frequencies and damping ratios of the structure.

	Mode	**1**	**2**	**3**	**4**	**5**	**6**	**7**
EMA	$\Omega_n\ [Hz]$	20.66	53.34	245.18	258.99	477.95	577.20	670.44
	$\zeta_n\ [\%]$	5.00	1.68	1.74	1.36	2.28	1.52	7.02
OMA	$\Omega_n\ [Hz]$	–	54.08	247.18	255.52	477.55	576.68	671.61
	$\zeta_n\ [\%]$	–	3.04	1.53	1.52	2.90	2.52	3.28
	Mode	**8**	**9**	**10**	**11**	**12**	**13**	
EMA	$\Omega_n\ [Hz]$	833.49	1045.75	1106.53	1158.67	1241.10	1461.06	
	$\zeta_n\ [\%]$	2.19	2.71	3.91	6.50	2.41	2.45	
OMA	$\Omega_n\ [Hz]$	834.11	1056.24	1106.80	1158.77	1240.23	–	
	$\zeta_n\ [\%]$	4.07	3.07	2.10	3.46	2.15	–	

Figure 5.1 shows modes 2 to 9 of the primary system (the first mode is a rigid body mode) as obtained via LMS Test.Lab for the EMA.

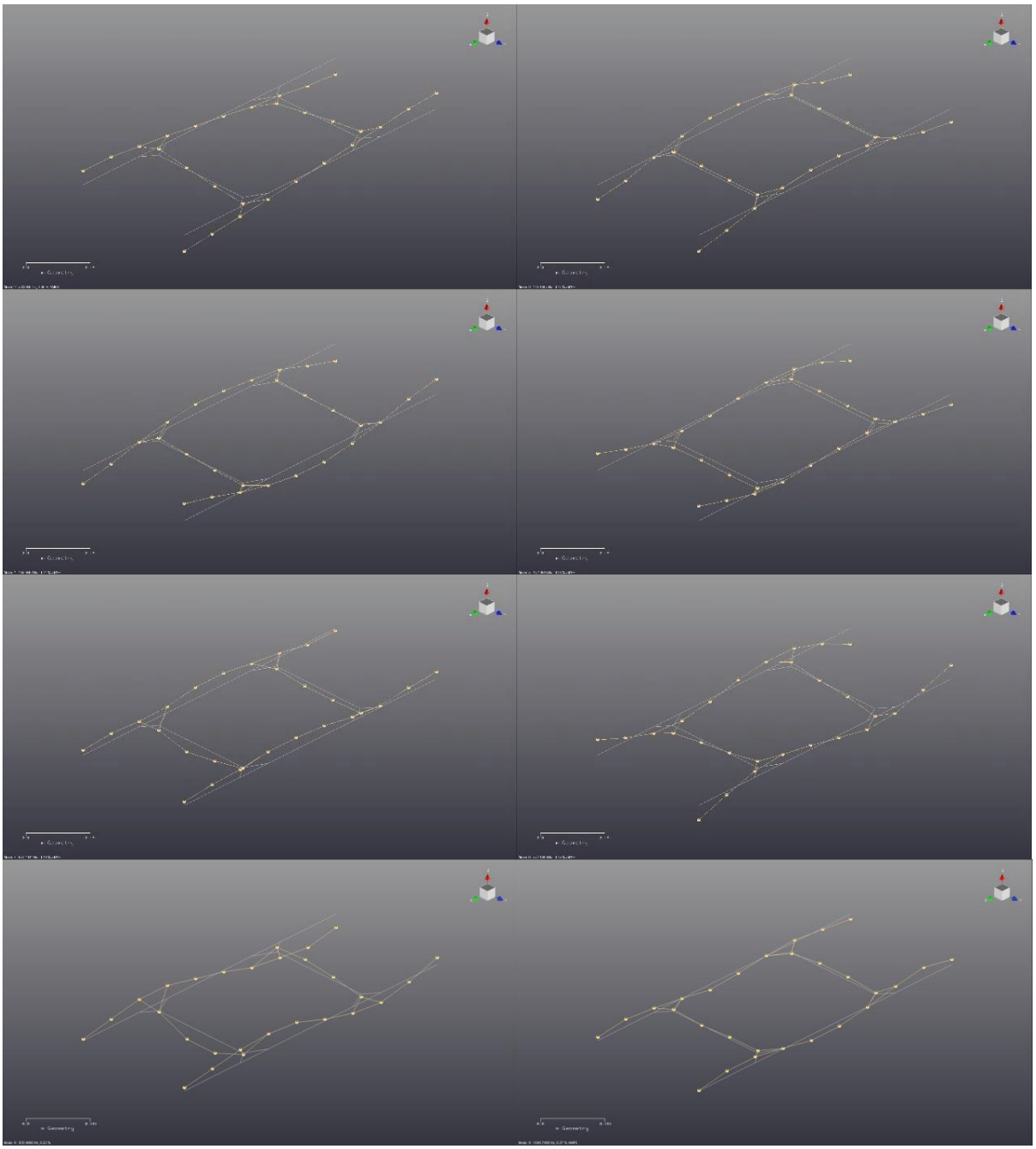

Figure 5.1 – First eight non rigid body modes of the structure.

Together with the modal matrices, the results of both analyses presented in this section are the input parameters for the optimization algorithm. The optimization results are the topic of the next section.

5.2. DESIGN PARAMETERS FOR THE EMA NEUTRALIZERS

The optimization process using the experimental modal parameters yields the values for the mass and the natural frequencies of each neutralizer. The dimensions of the resilient element are given by the form factor L from equation (3.88). In order to determine L, it is also necessary to calculate the shear modulus $G(\Omega_a)$ of the viscoelastic material in the resonance frequencies. The temperature was considered to be constant at 10° C (283 K).

Table 5.2 – DVN design parameters (EMA)

$\mathbf{m_a}$ [kg]	$\mathbf{\Omega_a^*}$ [Hz]	$\mathbf{G(\Omega_a)}$ [$\mathbf{10^6}$ $\mathbf{N/m^2}$]
0.0649	468.59	6.3995
0.0903	576.07	6.7540
0.2569	515.52	6.5597

Given the values from Table 5., it is possible to calculate the form factor of the resilient element:

$$L = \begin{Bmatrix} 0.0879 \\ 0.1751 \\ 0.4110 \end{Bmatrix} [m] \tag{5.1}$$

The viscoelastic material has a thickness of $h = 6.2\ [mm]$, and together with the form factor, it is possible to calculate the shear area:

$$A = Lh = \begin{Bmatrix} 0.5450 \\ 1.0857 \\ 2.5480 \end{Bmatrix} 10^{-3}\ [m^2] \tag{5.2}$$

As a construction choice, the neutralizer will have a circular form, in which the viscoelastic material will have a ring shape. The shear area is taken in the medium diameter of the ring that can be flattened to a rectangle - one side of which is the circumference of the ring and the other is the height of the ring

$$C = \frac{A}{t} = \begin{Bmatrix} 2.7248 \\ 4.3429 \\ 8.4934 \end{Bmatrix} 10^{-2} [m] \tag{5.3}$$

However, with these dimensions, it is not possible to bend the material into a ring. In order to solve this problem, the resilient layer can be built by arranging the viscoelastic material in parallel.

The equivalent stiffness of a parallel assembly is simply the sum of the individual stiffness. That means the material can be split in any number of parts and the stiffness will remain the same, as long as the total area remains the same. The height and operating

frequency remain the same. This allows the increase of radius by leaving empty spaces between the parts. These empty spaces also increase heat dissipation.

$$k_{eq} = k_1 + k_2 + \cdots + k_n \tag{5.4}$$

$$k_{eq} = \frac{A_1}{h} G(\Omega_a) + \frac{A_2}{h} G(\Omega_a) + \cdots + \frac{A_n}{h} G(\Omega_a) \tag{5.5}$$

$$A_1 \ldots A_n = \frac{A}{n} \tag{5.6}$$

$$k_{eq} = (A_1 + A_2 + \cdots A_n) \frac{G(\Omega_a)}{h} = n\left(\frac{A}{n}\right) \frac{G(\Omega_a)}{h} = \frac{A}{h} G(\Omega_a) \tag{5.7}$$

Among the many possible variations for DVN design, the chosen was a cylindrical construction, where the viscoelastic material is subject to shear deformation. This construction is easy, compact, and symmetrical. The symmetry allows the weight and stress to be evenly distributed along the rubber insert. The dimensions Di, De and T are chosen so that the mass of the ring is the mass from Table 5. The final assembly of the aluminum frame with the neutralizers is shown in Figure 5.3.

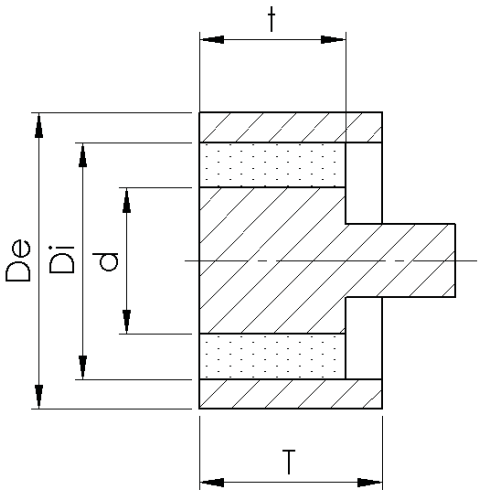

Figure 5.2 – Project of the DVN. Source: The Author.

Table 5.3 – Design parameters (EMA)

	$d\ [mm]$	$Di\ [mm]$	$De\ [mm]$	$t\ [mm]$	$T\ [mm]$
Neutralizer 1	20	32.4	39.75	10	20
Neutralizer 2	20	32.4	40.49	20	25
Neutralizer 3	25	37.4	52.89	30	30

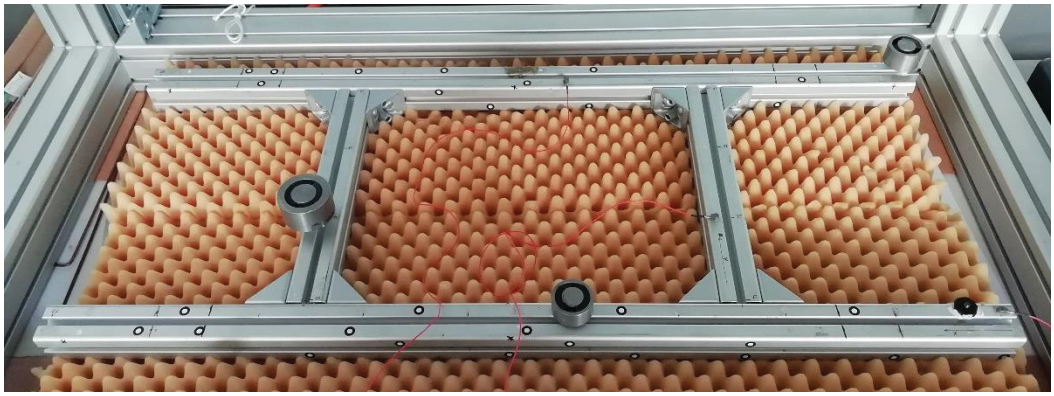

Figure 5.3 – Final assembly of the aluminum frame with neutralizers. Source: The Author.

5.3. DESIGN PARAMETERS FOR THE OMA NEUTRALIZERS

Like in section 5.2, the results of the operational modal analysis are used to design a set of neutralizers. However, given the characteristics of the modal parameters of OMA, some techniques used for the EMA design cannot be used in this chapter.

Since the modal mass is not known in OMA, the mass of the neutralizers cannot be determined by equation 4.116. Instead, the mass was chosen to be $200g$ each (about 5% of the total mass). For OMA, the input is not known, and so, the transfer function cannot be calculated; at least not by traditional methods. That means there is no theoretical curve to compare with experimental results. However, the experimental curves from the OMA design can be compared with those from the EMA design in order to determine its efficacy.

In this case, the optimization only provides the values for the natural frequencies, due to the fact that the mass was determined beforehand. The temperature was considered to be constant at 15° C (288 K).

Table 5.4 – DVN design parameters (OMA)

$\boldsymbol{\Omega_a^*}$ **[Hz]**	$\boldsymbol{G(\Omega_a)}$ **[10^6 N/m^2]**
287.44	7.1646
304.50	7.2787
442.00	8.0837

The total circumference for the new design is

$$C = \begin{Bmatrix} 4.8434 \\ 5.3502 \\ 10.1503 \end{Bmatrix} 10^{-2}[m] \tag{5.8}$$

The design is the same as presented in Figure 5.2, and the dimensions are presented in Table 5.5.

Table 5.5 – Design parameters (OMA)

	$\boldsymbol{d}$ **[mm]**	$\boldsymbol{Di}$ **[mm]**	$\boldsymbol{De}$ **[mm]**	$\boldsymbol{t}$ **[mm]**	$\boldsymbol{T}$ **[mm]**
Neutralizer 1	25	37.4	49.85	30	30
Neutralizer 2	25	37.4	49.85	30	30
Neutralizer 3	35	47.4	57.80	30	30

5.4. THEORETICAL RESULTS

Given the DVN design parameters, it is possible to calculate the modal matrix for the modified system using the theory presented in chapter 3 and, therefore, the response functions.

The response function depends on the point of excitation and the point where the response is measured. It can be interpreted as a matrix of response functions. Figure 5.4 shows all the response curves measured at point 1. This matrix is symmetrical ($\alpha_{ij} = \alpha_{ji}$), so only a few selected curves are necessary to convey the information representing the whole system. Figure 5.4 present the response curves measured at point 1, for the primary system and compound system. It can be seem that the expected result is a global reduction of vibration on the structure.

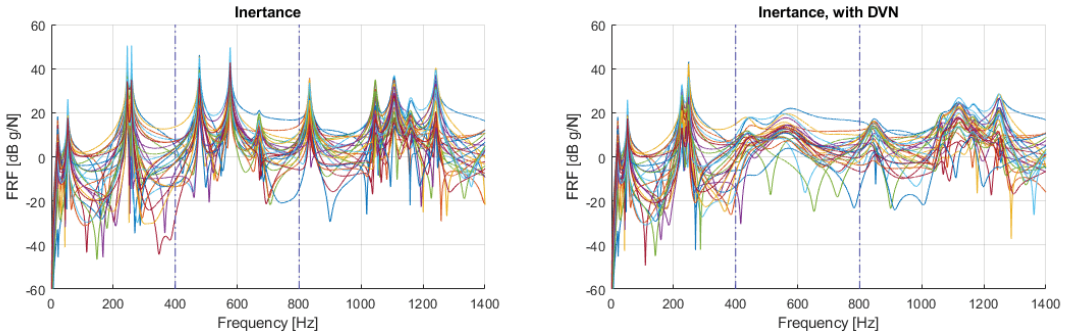

Figure 5.4 – All response functions measured in point 1 of (a) Primary system and (b) Compound system. Source: The Author.

The next set presented (Figure 5.5) are the response curves with excitation and measurement at the same point - being them point 1 - and the points where the neutralizers are installed (5, 11, and 26). The red dashed line is the response of the primary system, whereas the solid black line is the response of the compound system. The light blue dashed vertical lines are the frequency limits for control.

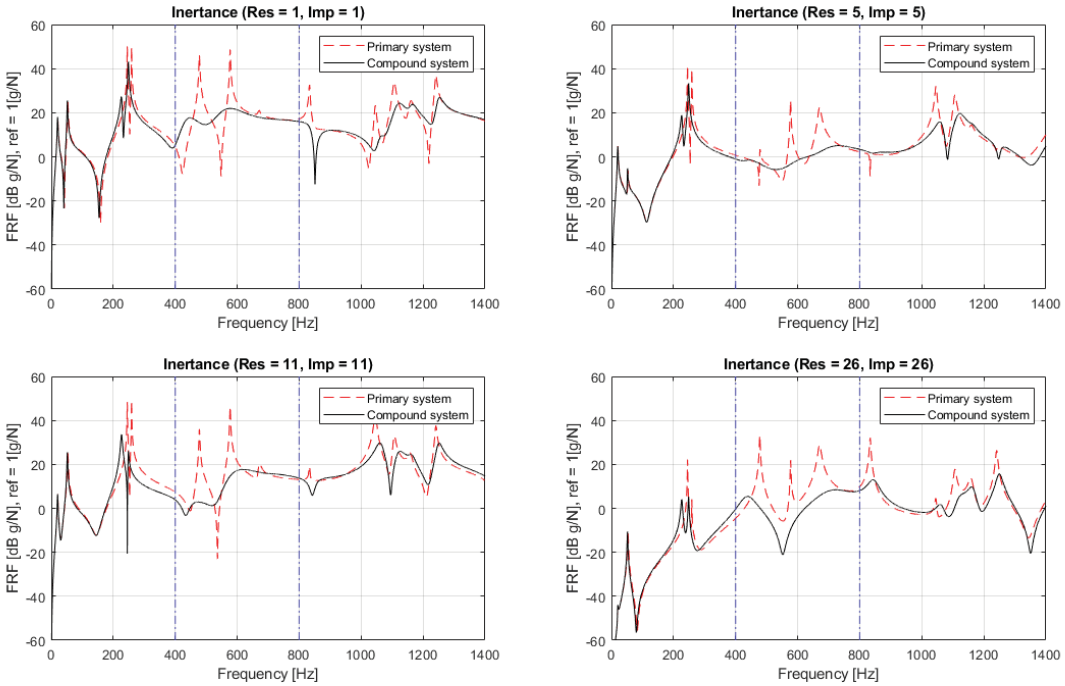

Figure 5.5 – Response curves at (a) 1-1, (b) 5-5, (c) 11-11, and (d) 26-26. Source: The Author.

The following set shows the response functions measured at point 1 and excited at the points where the neutralizers are installed (5, 11, and 26).

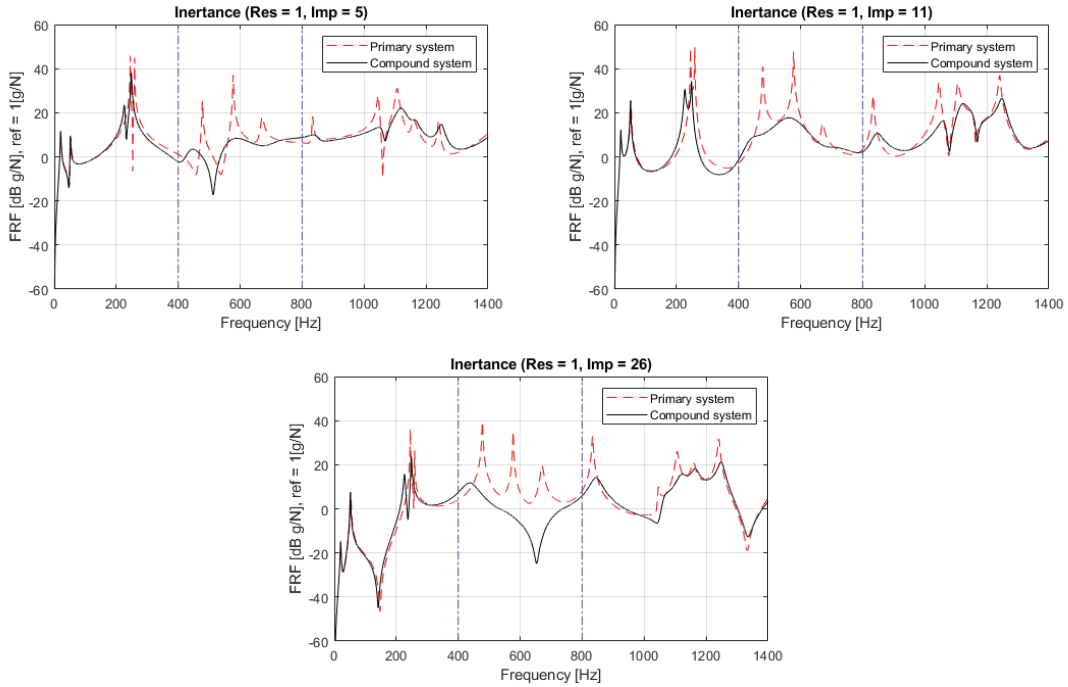

Figure 5.6 – Response curves at (a) 1-5, (b) 1-11, (c) 1-26. Source: The Author.

Figure 5.5 and Figure 5.6 show that the expected result does greatly reduce the vibration of the structure in the desired frequency interval for control. In this case, it is worth noting that the modes below the lower frequency limit ($400\ Hz$) suffer little or no vibration reduction, whereas vibration for the modes above the upper limit ($800\ Hz$) reduces to a certain extent. This is not always the case as this phenomenon depends on several factors, such as natural frequencies from both the primary system and the neutralizers, loss factor from the viscoelastic material, and mode shapes, to mention a few.

5.5. EXPERIMENTAL RESULTS FOR THE EMA NEUTRALIZERS

In experimental modal analysis, the impulse and response are measured, and so the FRF's can easily be calculated. With that, it is possible to compare the experimental results to the theoretical ones. Like before, the first set presented contains the response curves with excitation at point 1 and where the neutralizers are installed (5, 11, and 26). The measurement refers to point 1, where the accelerometer was installed. The red dash-dot line is the original response curve from the structure, the black dashed line is the response of the compound system (theoretical curve), whereas the solid blue line is the measure response of the compound system.

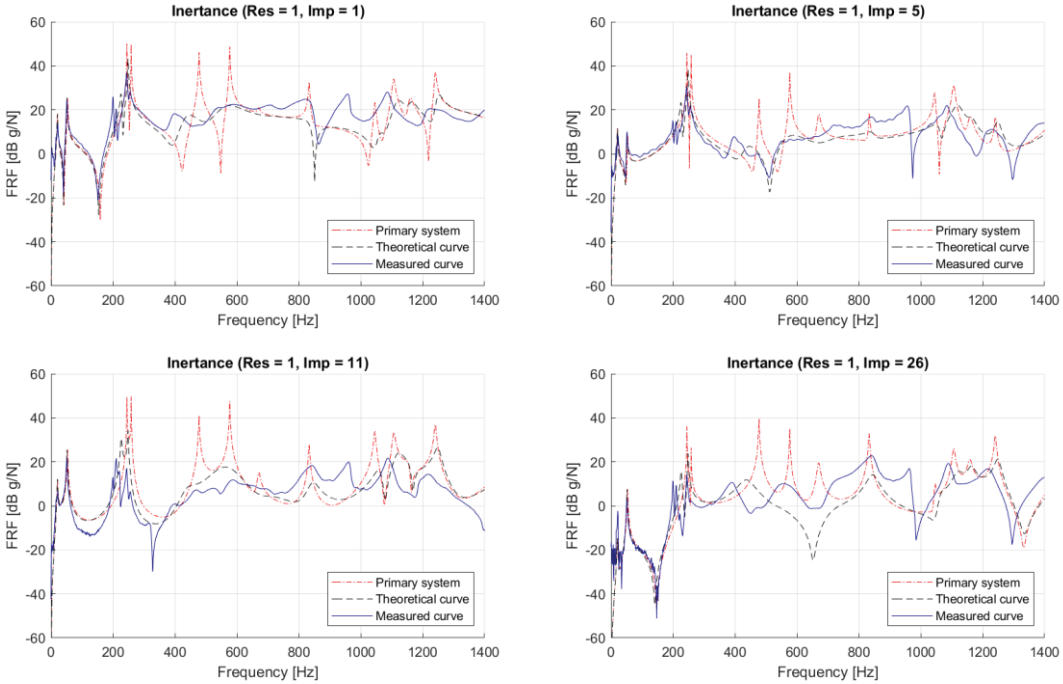

Figure 5.7 – Set of inertance curves measured at point 1. Source: The Author.

Accelerometers were also installed at the points 15 and 22. For each of these points another set of graphics will be presented, where the impulse will be at point 1 and where the sensor itself is installed. The first set is for the responses at point 15.

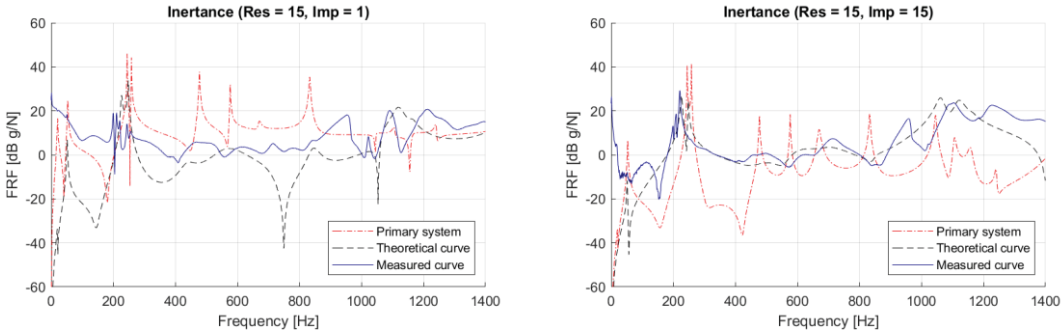

Figure 5.8 – Set of inertance curves measured at point 15. Source: The Author.

And again for the response at point 22 (Figure 5.9).

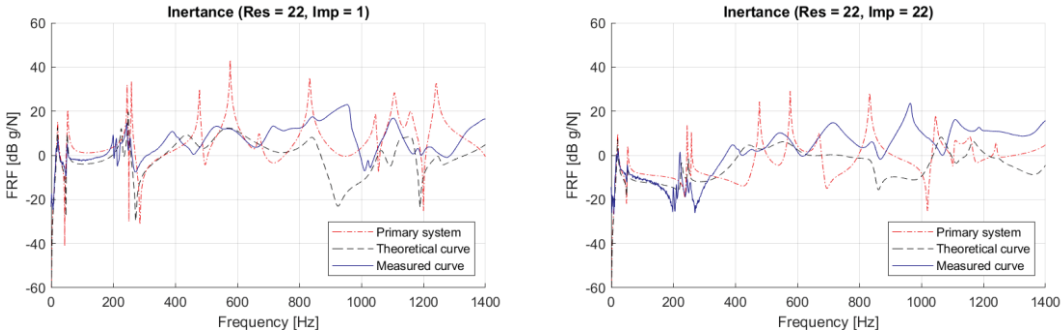

Figure 5.9 – Set of inertance curves measured at point 22. Source: The Author.

It can be seen in Figure 5.7, Figure 5.8, and Figure 5.9 that the neutralizers have little or no influence in the modes below the lower frequency limit for control. This can be explained by the fact that the response in lower frequencies is dominated by stiffness, and this design of DN's does modify the stiffness of the structure. In the control band, it is possible to see that the reduction is very close to what was predicted.

An interesting phenomenon occurs on higher frequencies. The reduction is not as high as predicted, and in some cases, it is possible to identify a resonance where an anti-resonance was predicted. The main driving factor for this involves the design choice of the neutralizers and a small limitation of the algorithm. Even though the algorithm takes into consideration the vibrating mass, it does not consider the mass of the metal core that serves as a base for the neutralizer. Other factors may also have affected the results, such as temperature, build tolerance, and pre-load (bending) of the viscoelastic material.

In the curves presented in Figure 5.8, the measured response greatly differs from the theoretical curve at frequencies lower than $100\ Hz$. This can be explained by the presence of a modal node at that point (or near it), which causes the response to be very low, so the actual measured signal is mostly noise in that frequency range. However, at higher frequencies, in particular at the control band, the curves are very similar, showing the efficacy and accuracy of the proposed method.

5.6. EXPERIMENTAL RESULTS FOR THE OMA NEUTRALIZERS

Even though OMA was performed at this stage of the work, which implies that obtaining a FRF would not be possible in this situation, FRF's were measured in order to compare the results with EMA.

The equivalent sets of graphics are presented. The red dash-dot line is the original response curve from the structure, and the solid blue line is the measure response of the compound system. The absence of a theoretical curve is explained by the fact that it is not possible to calculate an FRF from OMA parameters, as mentioned before.

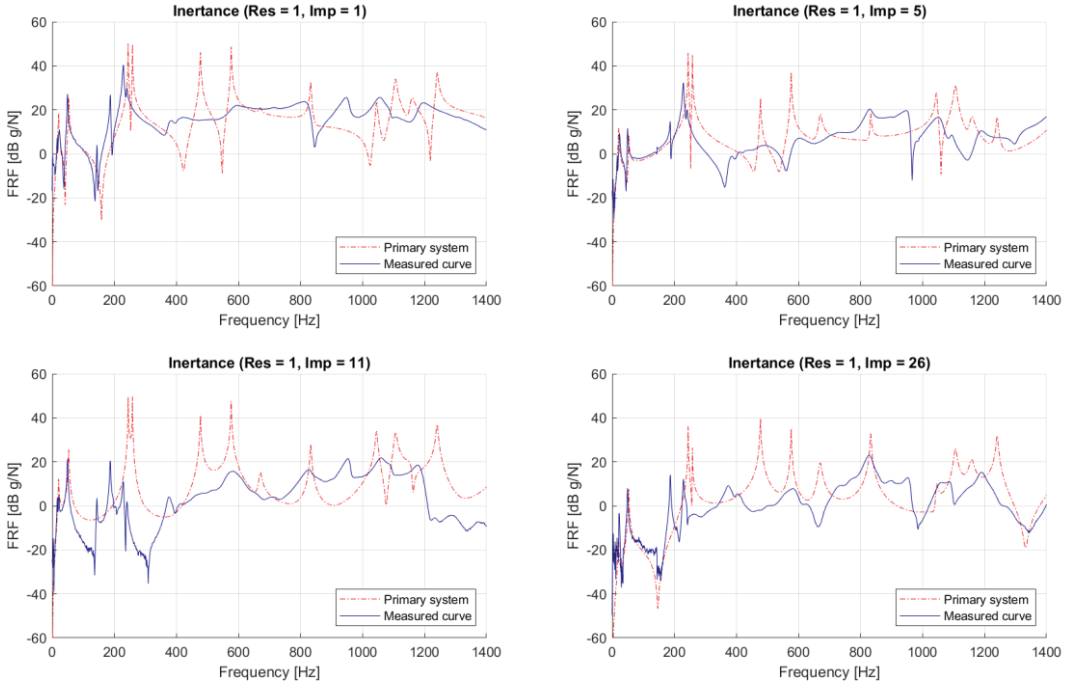

Figure 5.10 – Set of inertance curves measured at point 1 (OMA). Source: The Author.

Just as in the previous case, there is a significant reduction of vibrations on the chosen control, whereas the reduction is less significant outside it. Unlike the EMA case, it is possible to see a greater effect on the natural frequencies, especially below $400\ Hz$. This can be easily explained by the increased mass of the neutralizers.

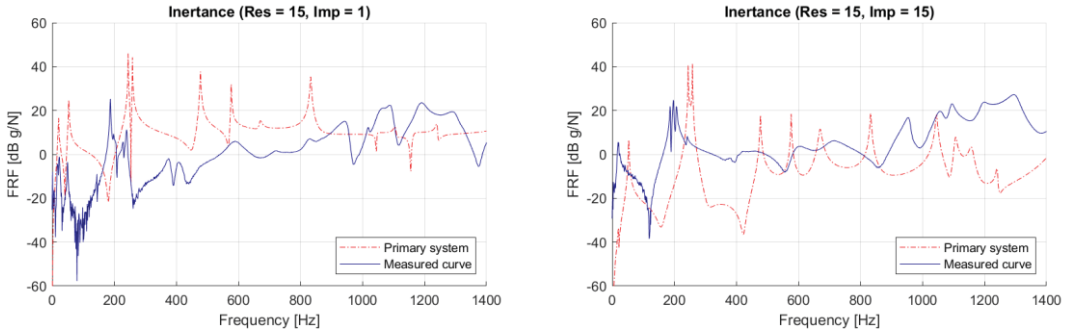

Figure 5.11 – Set of inertance curves measured at point 15 (OMA). Source: The Author.

Figure 5.11 it shows the responses at point 15. The effects of the neutralizer on the lower frequencies are clearer. It is also possible to see that the signal contains a lot of noise with the impulse at point 1.

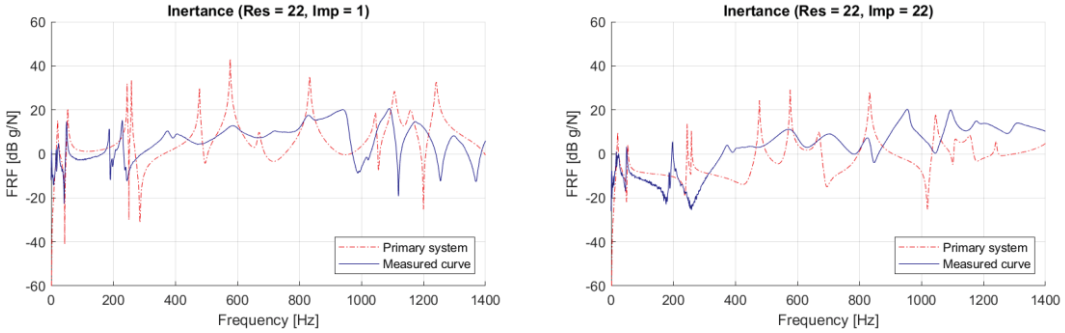

Figure 5.12 – Set of inertance curves measured at point 22 (OMA). Source: The Author.

5.7. COMPARISON WITH EXPERIMENTAL MODAL ANALYSIS

Section 6.2 shows the graphics comparing the response curves of the unmodified primary system with the curves of the compound system with DN using operational modal parameters. They show that it is possible to use OMA results to design DN's. However, in order to show that OMA parameters are a viable alternative to EMA parameters, the results of both designs must be compared.

In this section, only the graphics of the measured response curves of the compound system are presented. The curve in black is for the OMA design, while the one in red is for the EMA design.

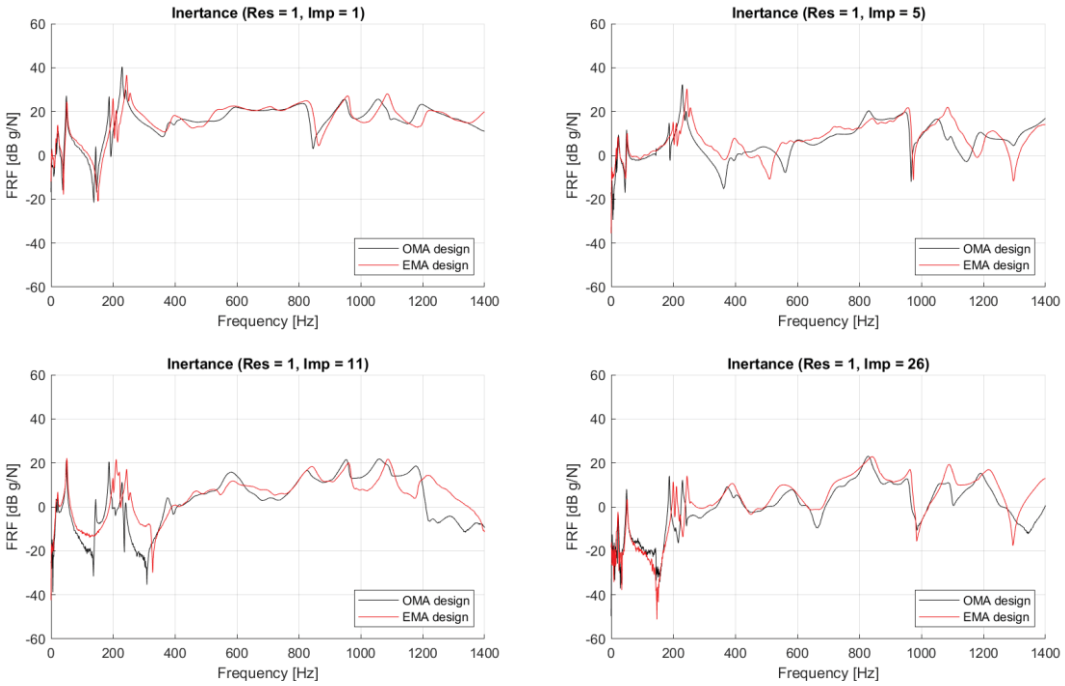

Figure 5.13 – Comparison of inertance curves measured at point 1. Source: The Author.

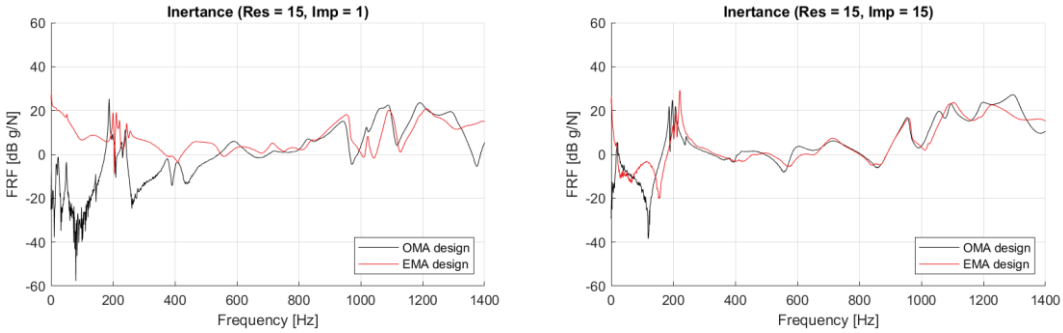

Figure 5.14 – Comparison of inertance curves measured at point 15. Source: The Author.

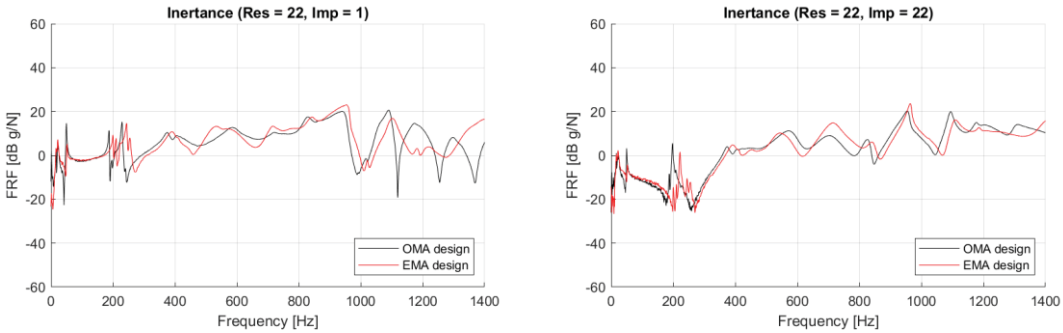

Figure 5.15 – Comparison of inertance curves measured at point 22. Source: The Author.

Analyzing the graphics in Figure 5.13, Figure 5.14, and Figure 5.15, it can be observed that the responses obtained using both EMA and OMA suffer a significant reduction in vibration levels. Not only that, but the answers are quite similar. A simple explanation is that OMA modes are proportional to EMA modes, that is, they have the same form, but with different amplitudes. In such a way that

$$[\psi_1\ \psi_2 \dots \psi_n] = [\kappa_1\phi_1\ \kappa_2\phi_2 \dots\ \kappa_n\phi_n] \tag{5.9}$$

where ψ_i are the non-normalized modes of OMA, ϕ_i are the normalized modes of EMA and κ_i are scaling factors of each mode ϕ_i. Thus, when using the operational modal parameters for the design of NDV's, vector $P(\Omega)$ becomes

$$\tilde{P}(\Omega) = \begin{Bmatrix} \kappa_1^2 P_1 \\ \kappa_2^2 P_2 \\ \vdots \\ \kappa_n^2 P_n \end{Bmatrix} \tag{5.10}$$

If $\kappa_1 \approx \kappa_2 \approx \cdots \approx \kappa$, then $\tilde{P}(\Omega) = \kappa^2 P(\Omega)$, and the objective function becomes $\tilde{f}(x) = \kappa^2 f(x)$. It is a known property of optimization that when an objective function is multiplied by a constant, its minima points do not change.

6. CONCLUSION

Initially the methodology for optimal design of NDV's - which assumes that the modal input parameters are normalized by mass - was reviewed and implemented. This methodology takes advantage of the concept of ‘generalized equivalent parameters’, which allows for a reduced computational time, a broadband control, and a generalized design for the neutralizers. It was theorized that this methodology is not dependent on the modal mass.

Experimental and operational modal analyses were performed on the aluminum frame structure. The results were used as input parameters for the methodology to design two sets of neutralizers, one for each analysis. Then, the neutralizers were attached to the structure, and the response of the compound system was measured for the two cases. These responses are the parameters that were used to determine the efficacy of the method and to see whether the methodology is viable using operational modal parameters.

The results obtained show that the neutralizers can be designed without the knowledge of the modal mass. However, the methodology for determining the mass of the neutralizers does depend on the modal mass, so a different approach had to be adopted. Then, the same methodology was used for the optimal design of NDVs using the non-normalized modal parameters obtained via OMA. Finally, the results obtained by analyzing the inertance curves for both designs were compared.

It can be observed that the responses for the two different designs are quite similar, although the masses of the NDVs are significantly different (and, therefore, so are the resonant frequencies). This indicates that yes, it is possible to use the same methodology for both EMA and OMA modal parameters, since the methodology is dependent on the mode shape regardless of its scaling factor.

REFERENCES

ARORA, J. S. **Introduction to Optimum Design**. 4th ed. San Diego: Elsevier. 2016.

BAGLEY, R. L. and TORVIK, P. J. A generalised derivative model for an elastomer damper. **Shock and Vibration Bulletin**. v. 49, p. 135-143. 1979.

BAGLEY, R. L. and TORVIK, P. J. A Theoretical Basis for the Application of Fractional Calculus to Viscoelasticity. **Journal of Reology.** v. 27, n. 3, p. 201-210. 1983.

BAGLEY, R. L. and TORVIK, P. J. On the fractional calculus model of viscoelastic behavior. **Journal of Reology.** v. 30, n. 1, p. 133-155. 1986.

BAVASTRI, C. A. **Redução de Vibrações de Banda Larga em Estruturas Complexas por Neutralizadores Viscoelásticos**, PhD Thesis, Universidade Federal de Santa Catarina, Brazil. 1997.

BAVASTRI, C. A. and ESPÍNDOLA, J. J. Modal Reduction of Vibrations by Dynamic Neutralizers in a Frequency Range – A Generalized Approach. **Proceedings of 4th DINAME**, Caxambú, Minas Gerais, v. 1, p. 214 – 217, 1995.

BRENNAN, M. J. and DAYOU, J. Global Control of Vibration Using a Tunable Vibration Neutralizer. **Journal of Sound and Vibration**, v. 232(3), p. 585 – 600, 2000.

BRINCKER, R. Some Elements of Operational Modal Analysis. **Shock and Vibration**, v. 2014, 2014.

BRINCKER, R. and VENTURA, C. E. **Introduction to Operational Modal Analysis**. Wiley. 2015.

BRINCKER, R.; ZHANG, L. and ANDERSEN, P. Modal identification from ambient responses using frequency domain decomposition. **Proceedings of IMAC 18, the International Modal Analysis Conference**, San Antonio, TX, p. 625–630, 2000.

CASTRO, F. E. S.; BAVASTRI, C. A. A methodology for an optimal design of physical parameters, positions, and viscoelastic materials of simple dynamic absorbers for passive vibration control. **Journal of Vibration and Control**, v. 25(6), p. 1133-1147. 2019.

DAYOU, J. and BRENNAN, M. J. Global Control of Structural Vibration Using Multiple-Tuned Tunable Vibration Neutralizers. **Journal of Sound and Vibration**, v. 258(2), p. 345 – 357, 2002.

DE SOUSA, T. L. **Identificação Integrada de Propriedades Mecânicas de Materiais Viscoelásticos nos Domínios do Tempo e da Frequência Considerando a Influência da Temperatura**, PhD Thesis, Universidade Federal do Paraná, Brazil. 2018.

DEN HARTOG, J. P. **Mechanical Vibrations**. New York: McGraw-Hill. 1956.

ESPÍNDOLA, J. J. and SILVA, H. P. Modal reduction of vibrations by dynamic neutralizers: a generalized approach. **Proceedings of the 10th International Modal Analysis Conference**, San Diego, CA, p. 1367–1373, 1992.

ESPÍNDOLA, J. J.; MÉNDEZ, G. A.; LOPES, E. M. and BAVASTRI, C. A. On the Design of Optimum Systems of Viscoelastic Vibration Absorbers Based on the Fractional Calculus Model. **Proceedings of the 13th International Workshop on Dynamics & Control.** Wiesensteig, Germany. 2005a.

ESPÍNDOLA, J. J.; SILVA, H. P. and LOPES, E. M. O. A generalized fractional derivative approach to viscoelastic material properties measurements, **Applied Mathematics and Computation**, v. 164, n. 2, p. 493–506, 2005b.

ESPÍNDOLA, J. J.; BAVASTRI, C. A. and LOPES, E. M. O. On the Design of Optimum System of Viscoelastic Vibration Absorbers for a Given Viscoelastic Material. **Proceedings of the XII International Symposium on Dynamic Problems of Mechanics**. Ilhabela, SP, Brazil. 2007.

ESPÍNDOLA, J. J.; BAVASTRI, C. A. and LOPES, E. M. O. Design of Optimum System of Viscoelastic Vibration Absorbers for a Given Material Based on the Fractional Calculus Model. **Journal of Vibration and Control**. 14(9–10): 1607–1630, 2008.

EUGENI, M.; SALTARI, F.; COPPOTELLI, G. and DESSI, D. A method for the estimate of modal parameters of time-dependent aerospace structural systems using operational data. **Proceedings of the 7th International Operational Modal Analysis Conference**, Ingolstadt, 2017.

EWINS, D. J. **Modal Testing: Theory and Practice**, Research Studies Press Ltd., Somerset, England, 1984.

FRAHM, H. **Device for damping vibrations of bodies**. US Patent 989958A. Apr 1911.

GUILLAUME P., VERBOVEN P., VANLANDUIT S, VAN DER AUWERAER H. and PEETERS B.: A poly-reference implementation of the least-squares complex frequency domain-estimator. **Proceedings of the 21st International Modal Analysis Conference**, Kissimmee, FL, 2003.

HUANG, S. C. and LIN, K. A. A New Design of Vibration Absorber for Periodic Excitation. **Shock and Vibration**, v. 2014, 2014.

INMAN, D. J. **Engineering Vibration**. 4th ed. Pearson. 2014.

JONES, D. I. G., NASHIF, A. D. and STARGARDTER, H. Vibrating Beam Dampers for Reducing Vibrations in Gas Turbine Blades. **Journal of Engineering for Power**. p. 111-116, 1975.

KHATIBI, M.M., ASHORY, M.R., MALEKJAFARIAN, A. and BRINCKER, R. Mass-stiffness change method for scaling of operational mode shapes. **Mech. Syst. Signal Process.**, v. 26, p. 34-59, 2012

KIM, S. Y. and LEE, D. Identification of fractional-derivative-model parameters of viscoelastic materials from measured FRF's. **Journal of Sound and Vibration**. v. 324, p. 570-586, 2009.

KITTIS, L. Vibration Reduction over a Frequency Range. **Journal of Sound and Vibration**. v. 89, p. 559-569, 1983.

LOPEZ-AENLLE, M.; BRINCKER, R; and CANTELI, A.F. Some methods to determine scaled mode shapes in natural input modal analysis. **Proceedings of the International Modal Analysis Conference (IMAC)**, Orlando, FL, 2005

NASHIF, A. D. and JONES, D. I. G. A Resonant Beam Tuned Damping Device. **Journal of Engineering for Power**. p. 143-148, 1969.

NASHIF, A. D.; JONES, D. I. G. and HENDERSON, J. P. **Vibration Damping**. New York: John Wiley & Sons Inc. 1985.

NELDER, J. A. and MEAD, R. A. A Simplex method for function minimization. **The Computer Journal**. v. 7, p. 308-313. 1965.

OLIENICK FILHO, E. G. **Caracterização Dinâmica de Materiais Viscoelásticos Termoreologicamente Simples em Função dos Efeitos da Temperatura, Frequência e Pré-Carga**. PhD Thesis, Universidade Federal do Paraná, Brazil, 2018.

ORMONDROYD, J. and DEN HARTOG, J. P. Transactions of the American Society of Mechanical Engineers. **The theory of the dynamic vibration absorber.** v. 50, p. 9-22. 1928

OVERSCHEE, P. and DE MOOR, B. **Subspace identification for linear systems, theory, implementation, application**, Kluwer Academic Publishers, 1996.

PADOVAN, J. and GUP, Y. General response of viscoelastic systems modelled by fractional operators. **Journal of the Franklin Institute**. v. 325, n. 2, p. 247-275. 1988.

PARLOO, E.; VERBOVEN, P.; GUILLAUME, P. and VANOVERMEIRE, M. Sensitivity-based operational mode shape normalization. **Mech. Syst. Signal Process.**, v. 16, p. 757-767, 2002.

PRITZ, T. Frequency dependencies of complex moduli and complex Poisson's ratio of real solid materials. **Journal of Sound and Vibration**. v. 214, n. 1, p. 83-104. 1988.

RAO, M. D. Recent applications of viscoelastic damping for noise control in automobiles and commercial airplanes. **Journal of Sound and Vibration**. v. 262, p. 457-474, 2003.

RAO, S. **Mechanical Vibrations**. 4th ed. Pearson Prentice Hall. 2004.

SCHNEIDER, T. Application of operational modal analysis to industrial machinery and plants. **Proceedings of the 7th International Operational Modal Analysis Conference**, Ingolstadt, 2017.

SNOWDON, J. C. **Vibration and Shock in Damped Mechanical Systems**. New York: John Wiley & Sons Inc. 1968.

SNOWDON, J. C. and NOBILE, M. A. Beamlike Dynamic Vibration Absorbers. **Acustica**. v. 44, p. 98-108, 1980.

SNOWDON, J. C., WOLFE, A. A. and KERLIN, R. L. Beamlike Dynamic Vibration Absorbers. **Acustica**. v. 44, p. 98-108, 1980.

VAN OVERSCHEE, P. and DE MOOR, B. **Subspace Identification for Linear Systems: Theory-Implementation-Applications**. Dordrecht: Kluwer Academic Publishers. 1996.

APPENDIX A — NELDER MEAD ALGORITHM

A.1 — NOTATION

The following notation is used in describing operations of the algorithm:

x^C, f^C: centroid of n best points (side opposite to the worst vertex, and the corresponding function value.

x^E, f^E : expansion point and corresponding function value.

x^L, f^L : best point (point 1) and corresponding function value (smallest).

x^Q, f^Q : contraction point and corresponding function value.

x^R, f^R : reflected point and corresponding function value.

x^S, f^S : second worst point and corresponding function value.

x^W, f^W : worst point (point $n+1$) and corresponding function value (largest).

The algorithm starts by evaluating the function at the $n+1$ points of the simplex, and then arranging then in ascending order of value of the function, such that:

$$f_1 \leq f_2 \leq f_3 \leq \cdots \leq f_{n+1}$$

With the points properly arranged, the centroid of the n best points is calculated (all points, except the worst) by the following equation:

$$x^C = \frac{1}{n}\sum_{k=1}^{n} x^{(k)} \qquad \text{(A.1)}$$

A.2 — BASIC OPERATIONS

The first operation to be performed is 'reflection' (Figure A.1a). It is expected that point x^R obtained by reflecting x^W regarding the opposite face of the simplex will have a smaller function value. If this is the case, then the a new simplex is formed by rejecting x^W and replacing it with the new point x^R. The idea is that the simplex always moves away from the worst point. Mathematically, the reflection point x^R is a vector equation derived as:

$$x^R = x^W + (1+\alpha_R)(x^C - x^W) = (1+\alpha_R)x^C - \alpha_R x^W, with\ 0 < \alpha_R \leq 1 \qquad \text{(A.2)}$$

While $\alpha_R = 1$, the simplex is fully reflected, that means the new simplex has the same shape as the original. Otherwise, the simplex is only partially reflected.

If the reflection produces a better point, one can generally expect to reduce the function value even further by moving on in the same direction. This is achieved by the expansion operation that produces point x^E by replacing α_R from the reflection operation with the expansion parameter α_E, in that $\alpha_E > 1$ (Figure A.1b).

$$x^E = (1 + \alpha_E)x^C - \alpha_E x^W, with\ \alpha_E > 1 \quad \text{(A.3)}$$

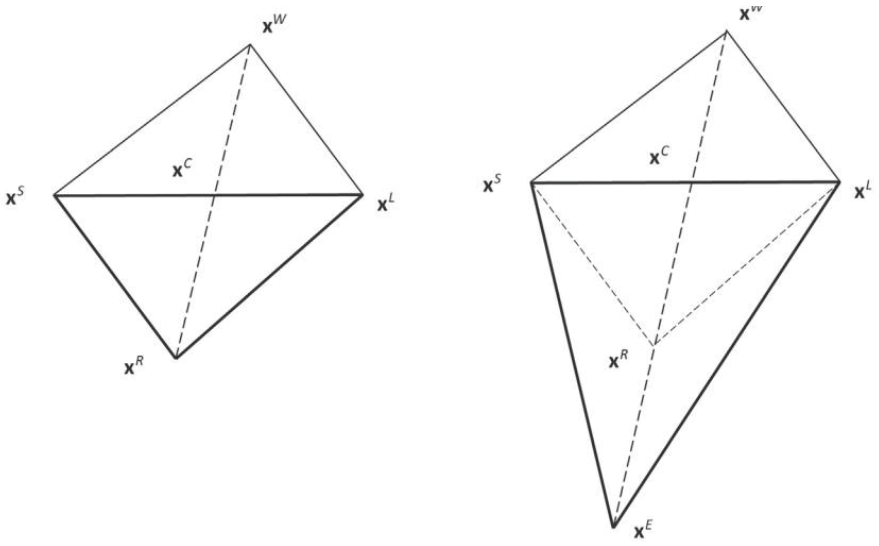

Figure A.1 – (a) Reflection of the worst pointx^W; (b) Expansion operation to x^E. Source: Arora (2016).

If the point obtained by reflection is not satisfactory, a contraction point x^Q along the direction x^C to x^R can be calculated by replacing α_R with a contraction parameter $-1 < \alpha_Q < 0$. There are two possible contraction operations, both shown in Figure A.2: an external contraction defined by equation A.4, or an internal contraction defined by equation A.5:

$$x^Q = x^R + \alpha_Q(x^R - x^C) = (1 + \alpha_Q)x^R - \alpha_Q x^C \quad \text{(A.4)}$$

$$x^Q = x^C + \alpha_Q(x^C - x^W) = (1 + \alpha_Q)x^C - \alpha_Q x^W \quad \text{(A.5)}$$

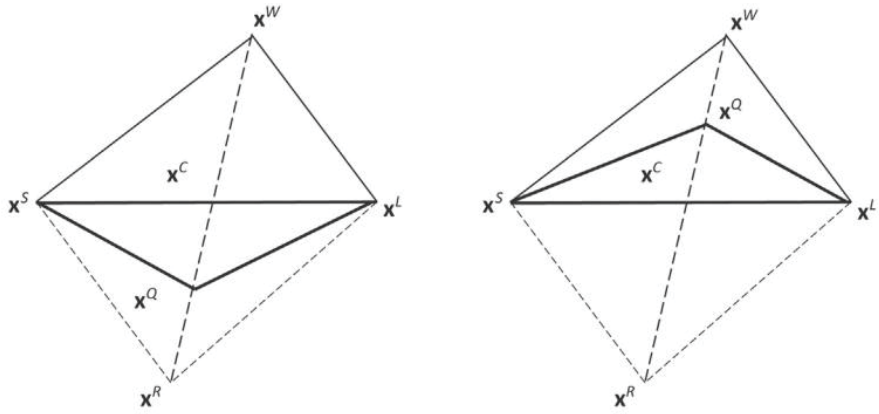

Figure A.2 – Contraction operation: (a) External; (b) Internal. Source: Arora (2016).

Another operation that can be performed by the algorithm is called ‘shrinking’. This operation shrinks the simplex towards the best point $x^{(1)}$. This operation differs from the others as it calculates several new points instead of just one.

$$x^{(j)} \leftarrow x^L + \delta\left(x^{(j)} - x^L\right);\ f_j = f\left(x^{(j)}\right);\ 0 < \delta < 1;\ j = 2, 3, \dots, n+1 \qquad \text{(A.6)}$$

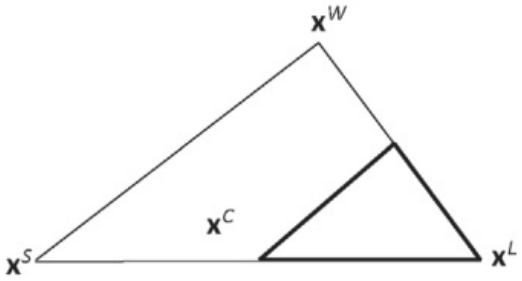

Figure A.3 – Shrinking operation of the simplex towards the best point. Source: Arora (2016).

A.3 — THE ALGORITHM

The Nelder-Mead algorithm is one of the best methods in the direct search class. This is one of the methods used in MATLAB; it is accessed by the *fminsearch* function. The parameters used by the software are $\alpha_R = 1$, $\alpha_E = 2$, $\alpha_Q = 0.5$ and $\delta = 0.5$.

To begin with, the algorithm generates an initial simplex, that has $(n + 1)$ points, or vertices. These are generated using a seed point (taken as $x^{(1)}$) and use that to generate the remaining n points based on displacement along the coordinate axes as:

$$x^{(j)} = x^{(1)} + \delta_j e^{(j)};\ j = 2, 3, \dots, n+1 \qquad \text{(A.7)}$$

Where δ_j is a step size in the direction of the j^{th} unit vector $e^{(j)}$. Once all the cost functions have been calculated for this initial simplex, they can be rearranged in ascending order, and the algorithm is ready to be initialized.

Table A.1 – The Nelder-Mead Algorithm. Adapted: Arora (2016).

The Nelder-Mead Algorithm
Step 1: Check for the termination criteria; if satisfied, stop the iterative process. Otherwise, for the simplex formed of $n + 1$ points, let x^W be the worst point and x^C be the centroid of the remaining n points. Let x^S be the second worst point of the simplex with the function value f^S. Compute the reflection point x^R using equation A.2.
Step 2: Evaluate the objective function value f^Rat x^R. If$f^L \leq f^R < f^S$, accept x^R as the replacement point and go to *step 6*. If $f^R > f^S$, go to *step 4* to perform contraction operation. If $f^R < f^L$, continue to *step 3* to perform expansion operation.
Step 3: *Expansion*: Calculate the expansion point x^E using equation A.3. Calculate the function value f^E at x^E. If $f^E < f^R$, accept x^E as the replacement point and go to *step 6*. If $f^E \geq f^R$, accept x^R as the replacement point and go to *step 6*.
Step 4: Contraction: If$f^S \leq f^R < f^W$, calculate x^Q (external contraction) using equation A.4. Evaluate the function value f^Q. If $f^Q < f^S$, then accept x^Q as the replacement point and go to *step 6*. Otherwise, go to *step 5*. If $f^R \geq f^W$, calculate x^Q (internal contraction) using equation A.5 and evaluate f^Q. If $f^Q < f^W$, accept x^Q as the replacement point and go to *step 6*. Otherwise, go to *step 5*.
Step 5: Shrink the simplex using equation A.6 and the corresponding objective function values. Rearrange the vertices of the simplex in the ascending order and return to *step 1*.
Step 6: Update the simplex by replacing x^W with the replacement point. Return to *step 1*.

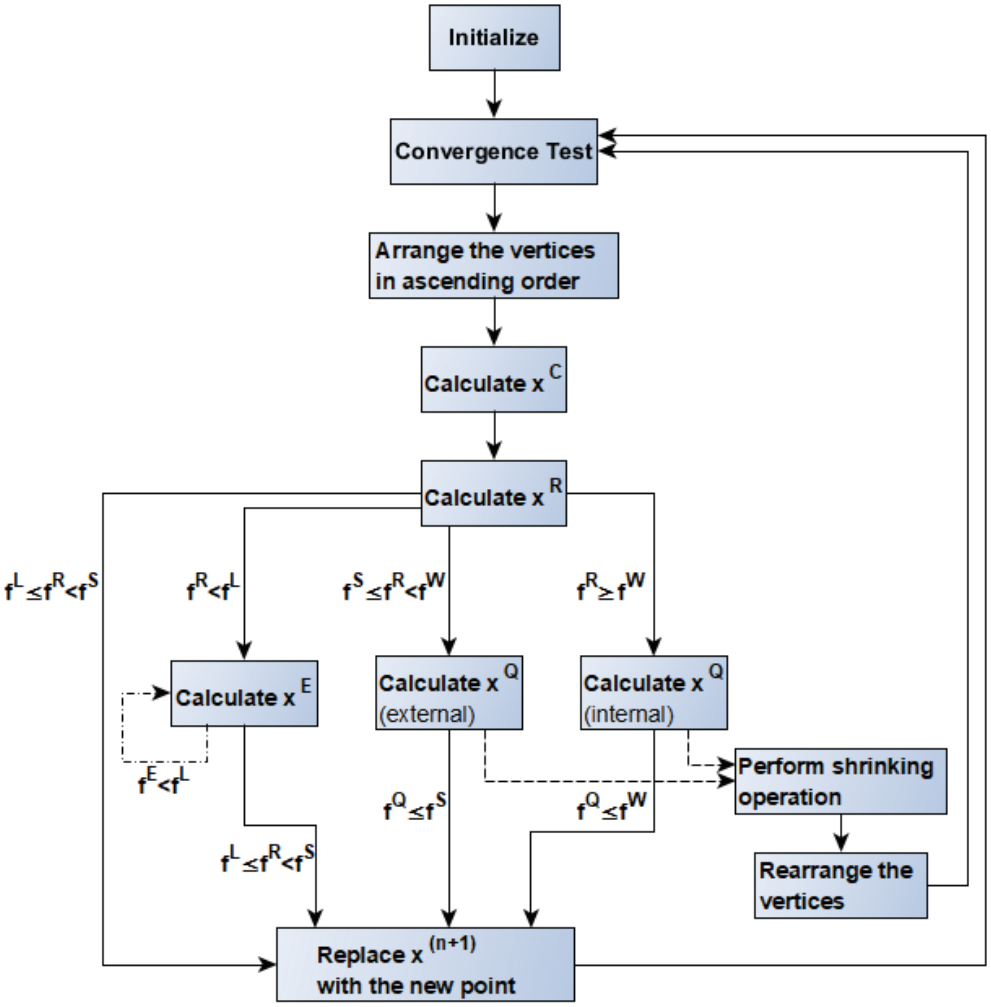

Figure A.4 – Diagram of the Nelder-Mead algorithm. Source: The Author.